https://doi.org/10.5194/essd-2024-483
Preprint. Discussion started: 18 December 2024

Open Access Earth System Science Data Discussions

Development of level 2 aerosol and surface products from cross-track scanning polarimeter POSP onboard GF-5(02) satellite

Cheng Chen[1], Xuefeng Lei[1], Zhenhai Liu[1], Haorang Gu[2], Oleg Dubovik[3], Pavel Litvinov[4], David Fuertes[4], Yujia Cao[1,5], Haixiao Yu[1,5], Guangfeng Xiang[1], Binghuan Meng[1], Zhenwei Qiu[1], Xiaobing Sun[1], Jin Hong[1], Zhengqiang Li[2]

[1] Anhui Institute of Optics and Fine Mechanics, Hefei Institutes of Physical Science, Chinese Academy of Sciences, Hefei 230031, China
[2] State Environment Protection Key Laboratory of Satellite Remote Sensing, Aerospace Information Research Institute, Chinese Academy of Sciences, Beijing 100101, China
[3] Univ. Lille, CNRS, UMR 8518 - LOA - Laboratoire d'Optique Atmosphérique, F-59000 Lille, France
[4] GRASP-SAS, Satellite Remote Sensing Development, Lille 59260, France
[5] University of Science and Technology of China, Hefei 230036, China

Correspondence to: Zhengqiang Li (lizq@radi.ac.cn)

Abstract. Development of long-term continues, consistent and high-quality satellite remote sensing aerosol and surface products is crucial to constrain climate models and improve our understanding on climate change. Particulate Observing Scanning Polarization (POSP) is the first space-borne multi-spectral (UV-VIS-NIR-SWIR) cross-track scanning polarimeter dedicated to complement Directional Polarimetric Camera (DPC) multi-angular polarimetric measurements and perform synergetic observations namely the Polarization Cross-Fire suite (PCF) onboard Chinese Gaofen series GF-5(02) satellite. The POSP unique single-viewing spectral (UV-VIS-NIR-SWIR) high-precision polarimetric measurements provide rich information for atmospheric aerosol and surface characterization. Here we developed aerosol and surface products from POSP/GF-5(02) based on the Generalized Retrieval of Atmosphere and Surface Properties (GRASP)/Models approach. The detailed retrieval approach and processing scheme are provided. The baseline level 2 product was generated for the first 18 months POSP measurements from December 2021 to May 2023 and publicly available and registered at doi.org/10.57760/sciencedb.14748. The obtained POSP/GF-5(02) aerosol and surface products are validated and intercompared with ground-based AERONET reference aerosol dataset and other independent satellite products, such as NOAA-20 VIIRS/DB aerosol product and MODIS MCD43 surface product. The results show generally good consistency of POSP products with AERONET, VIIRS/NOAA-20 aerosol dataset and MODIS surface product. Moreover, it is possible to conclude the developed POSP product includes reliable estimates of not only total Aerosol Optical Depth (AOD), but also detailed properties of aerosol such as aerosol size, absorption, layer height, type, etc., as well as full surface Bidirectional Reflectance Distribution Function (BRDF), Bidirectional Polarization Distribution Function (BPDF), and black-sky, white-

https://doi.org/10.5194/essd-2024-483
Preprint. Discussion started: 18 December 2024

sky albedos and Normalized Difference Vegetation Index (NDVI). These parameters are of high importance to constrain the Earth-atmosphere radiation budget. The retrieval of these properties seems to be possible due to the polarimetric capabilities and wide UV-VIS-NIR-SWIR spectral range of from POSP observations and advances of used GRASP/Models retrieval approach. Finally, some potential improvements for POSP level 1 to level 2 processing chain are identified, and limitations and lessons learned are discussed.

Short Summary. POSP on board GF-5(02) satellite is the first space-borne UV-VIS-NIR-SWIR multi-spectral cross-track scanning polarimeter. Due to wide spectral range and polarimetric capabilities, POSP measurements provide rich information for aerosol and surface characterization. We present the aerosol/surface products generated from POSP first 18 months of operation using GRASP/Models, including spectral AOD, AODF, AODC, and AE, SSA, scale height, full surface BRDF, BPDF, black-/white-sky albedos, NDVI.

1 Introduction

Satellite remote sensing provides an important source of data for dealing with the climate change challenges as well as monitoring environmental health. Therefore, the accumulation of high-quality long-term consistent remote sensing observational data has been paid more and more attention. Especially for climate change studies, the establishment of long-term and high-precision satellite remote sensing products, despite of huge challenges, is particularly important for reducing the uncertainty of climate change assessments (IPCC, 2021). Space agencies and even private companies are launching or planning to launch an increasing number of Earth-observing sensors. In particular, polarimetric remote sensing is widely regards as one of the best technologies for detecting atmospheric aerosols and clouds (Dubovik et al., 2019, 2021b; Hansen et al., 1997; Mishchenko et al., 2004). The deployment of the first multi-angular polarimeter (MAP) payload POLDER (Polarization and Directionality of the Earth's Reflectances) series (POLDER-1, -2 and -3) (Bréon et al., 2011; Deschamps et al., 1994; Tanré et al., 2011) developed by French national space agency (CNES), was followed by HARP-2 (Hyper-Angular Rainbow Polarimeter) and SPEXOne (Spectro-Polarimetric Experiment) recently launched on NASA's PACE (Plankton, Aerosol, Cloud, ocean Ecosystem) mission (Hasekamp et al., 2019; Martins et al., 2018; Remer et al., 2019a, b). In addition, the first commercial multi-angular cub-sat polarimeter of GAPMAP series has been launched by GRASP-Earth (Fuertes et al., 2023; Martins et al., 2024). The richness of multi-angular polarimetric is evident and demonstrated in numerous applications (Cairns et al., 2009; Chen et al., 2020, 2022a; Dubovik et al., 2011, 2019; Fu et al., 2020; Fu and Hasekamp, 2018; Gao et al., 2019; Hasekamp et al., 2024, 2011; Knobelspiesse et al., 2020; Waquet et al., 2009; Xu et al., 2016, 2017a, b). At the same, the community also recognizes the challenges in extracting the large number of parameters from polarimetric observations (e.g. Dubovik et al., 2019; Chen et al., 2020). Therefore, in order to leverage the information richness of multi-angular polarimetric measurements on a global scale releasing different levels of products, and sharing the successes and challenges with the broader community is crucial.

https://doi.org/10.5194/essd-2024-483
Preprint. Discussion started: 18 December 2024

China has traditionally prioritized the development of Earth observation technologies and it has recently launched several payloads with polarimetric capabilities. Most of these sensors were designed and developed by the Anhui Institute of Optics and Fine Mechanics, Chinese Academy of Sciences (CAS) (Chen et al., 2021b; Li et al., 2018, 2022b, c, d). However, the past, past efforts were focused on the development of instruments, while development of user-end products, and in depth product analysis was lacking. For example, the Directional Polarimetric Camera (DPC), which is the first POLDER-like Chinese operational MAP sensor, has been launched on-board GaoFen-5 (GF-5) satellite in 2018 (Li et al., 2018) and several similar instruments are deployed on different platforms afterwards. There several case studies (regional or short-term) that use the data to determine aerosol and cloud properties have been published (Chen et al., 2021a; Ge et al., 2022; Jin et al., 2022; Lei et al., 2023; Li et al., 2021, 2022a; Shang et al., 2020; Wang et al., 2022; Yu et al., 2024; Zhang et al., 2023), however reliable information about the released global product as well as demonstration of their use for environment and climate applications is very limited.

In this study, we will focus on the development of global aerosol and surface products from a new polarimeter (POSP), the first space-borne UV-VIS-NIR-SWIR multi-spectral cross-track scanning polarimeter, onboard GF-5(02) satellite. The GRASP/Models approach, which has previously been successfully applied to multi-angle polarimeter (Chen, et al., 2020, Dubovik et al., 2021b, etc.) and multi-spectral spectrometer (UV-VIS-NIR-SWIR) (Litvinov et al., 2024 and Chen et al., 2024), is adapted to process POSP single-viewing UV-VIS-NIR-SWIR polarimeter measurements. In the previous development of TROPOMI/Sentinel-5p aerosol and surface products, within the framework of ESA S5p+Innovation AOD/BRDF project (Litvinov et al., 2022), we have demonstrated that the possibility for extend aerosol and surface characterization from single-view UV-VIS-NIR-SWIR measurements with properly constrained forward models and advanced retrieval algorithm (Litvinov et al., 2024; Chen et al., 2024a). We describe the POSP/GF-5(02) Level 1 measurements and global aerosol/surface datasets used in this study in Section 2. Section 3 describes the POSP aerosol and surface retrieval scheme and the Level 2 product specification. Section 4 illustrates the preliminary validation and evaluation of POSP Level 2 aerosol and surface product. The study is concluded in Section 5 with a summary and discussion of the lessons learned.

2 Data description

In this section, the POSP/GF-5(02) satellite Level 1 measurements and the independent ground-based and space-borne aerosol and surface datasets used in this study are described.

https://doi.org/10.5194/essd-2024-483
Preprint. Discussion started: 18 December 2024

2.1 Single-viewing scanning polarimeter POSP/GF-5(02) Level 1 data

Gaofen (GF) is a series of Chinese civilian remote sensing satellites specifically for China's high resolution Earth observation system (Chen et al., 2022c; Gu and Tong, 2015; Tong et al., 2016). Among them, GF-5 satellite is designed and dedicated for atmospheric detection and environment monitoring, including aerosol, cloud, water vapor, ozone as well as tracer gases. The first GF-5(01) satellite was launched on May 8, 2018. GF-5(01) carries 6 payloads, specifically Directional Polarization Camera (DPC), Environment Monitoring Instrument (EMI), Greenhouse-gases Monitoring (GMI), Atmospheric Infrared Ultra-spectral Sensor (AIUS), Visual Infrared Multispectral Sensor (VIMS) and Advanced Hyperspectral Imager (AHSI). GF-5(01) satellite continued working until March 2021. Subsequently, the second GF-5(02) satellite was launched on September 7, 2021. Generally, GF-5(02) keeps similar design with GF-5(01). In order to enhance the atmospheric detection capability, GF-5(02) deployed a new Particulate Observing Scanning Polarization (POSP) that is a cross-track scanning polarimeter to complement DPC and perform synergetic observations, namely the Polarization Cross-Fire suite (Li et al., 2022d). The original POSP design idea came from NASA Aerosol Polarimetry Sensor (APS) that was an along track scanning polarimeter and lost during unsuccessful launch of Glory mission in 2011 (Dubovik et al., 2019; Mishchenko et al., 2007). POSP is the first space-borne multi-spectral cross-track scanning polarimeter, covering UV-VIS-NIR-SWIR spectrum (Lei et al., 2020). Specially, an on-board calibration device is designed for POSP to perform on-orbit solar diffuse reflector-based radiometric calibration as well as polarimetric calibration. Hence, it is expected to obtain high-precision polarimetric measurements from POSP achieving cross-calibration between DPC and POSP (Lei et al., 2023). Table 1 summaries the POSP/GF-5(02) main sensor characteristics and spectral channels used in this study.

Table 1. Instrument characteristics for POSP onboard GF-5(02) satellite

Spectrum	UV	VIS				NIR	SWIR		
Central band (nm)	381	410	442	489	670	865	1380	1611	2254
Polarization	I/Q/U								
Expected accuracy	ΔI 5% (UV-NIR-NIR); ΔI 6% (SWIR); ΔDoLP 0.005								
L1B Spatial Sampling	Nadir: 6.4 km								
Spectral resolution (nm)	20					40	60	80	
Rotational period (sec)	0.97911								
Scanning width	1850 km								

Our development of the Level 2 aerosol and surface processing starts from the POSP Level 1B TOA measurements. Before re-griding Level 1B onto Level 1C 10 km x 10 km grid, we use 3 consecutive steps to filter Level 1B data for aerosol and surface retrieval. Figure 1 shows the schematic diagram to illustrate the POSP data preprocessing from Level 1B to Level 1C for aerosol and surface retrieval.

https://doi.org/10.5194/essd-2024-483
Preprint. Discussion started: 18 December 2024

120

Step 1: Skip left and right 10 pixels at the edges of each swath.

The spatial resolution of POSP L1B pixel is approximately 6.4 km at nadir, and spatial sampling size become larger as the scan gets closer to the edge of the track (Figure 1). The POSP field of view is +/- 50°, orbit height is at ~706 km, therefore the pixel size at the edge is approximately 20.7 km. According to the recommendation from Level 1 data team, we simply
125 skip 10 pixels at the edges of each swath and proceed with 10 km Level 2 aerosol and surface retrieval.

Step 2: Cloud mask

Although the delivered POSP L1B data come with cloud identification, but some evident misclassifications are observed and it is with limited performance. We apply three additional conditions to filter cloudy pixels based on simply threshold
130 methods. Specifically, TOA reflectance R (1380 nm) < 0.02 is used to filter possible cirrus cloud. Then, the MODIS spatial variability method (3x3 window standard deviation) is used (Martins et al., 2002) and the threshold is slightly adjusted for POSP. We use 3x3_STD_R (412 nm) <0.03 over land, and 3x3_STD_R (865 nm) <0.03 over ocean. In addition, we use a one-pixel buffer zone for possible cloud shadow. Any pixel next to an identified cloudy pixel is removed for aerosol and surface retrieval. Overall, there is a big potential for improving cloud identification for POSP Level 1B data generation,
135 especially the polarimetric measurements are not used for the moment. The snow/ice mask is not used in this study, and part of snow/ice pixels can be removed in the cloud procedure, and others may affect our Level 2 aerosol and surface retrieval.

Step 3: Ocean glint mask

The ocean sun-glint mask is achieved by applying threshold on the glint angle (θ_g) using solar, view zenith angles (θ_s and
140 θ_v) and their relative azimuth angle ($\Delta\phi$) (see Eq. 1) (Cox and Munk, 1954). Small glint angle indicates higher probabilities of sun-glint. In this study, each ocean pixel with glint angle smaller than 40 degree is filtered.

$$\cos\theta_g = \cos\theta_v\cos\theta_s - \sin\theta_v\sin\theta_s\cos\Delta\phi \quad (1)$$

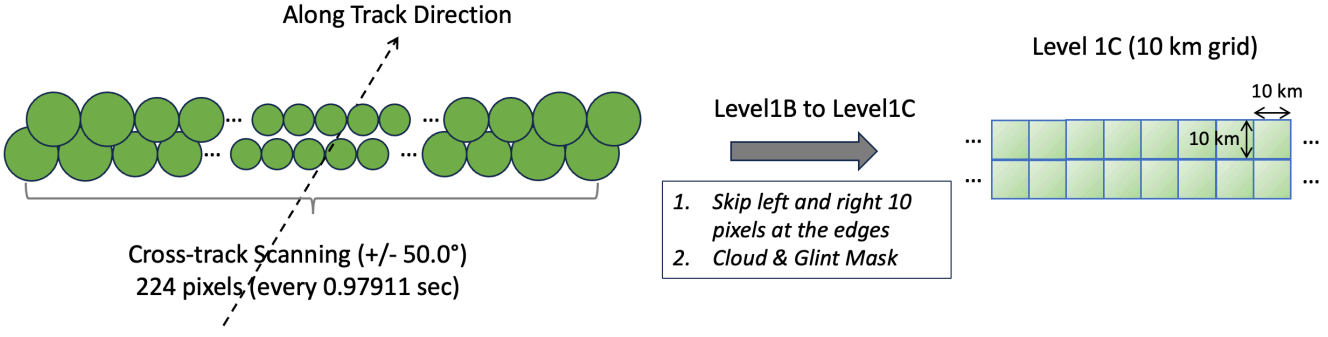

145

Figure 1. Schematic diagram to illustrate POSP data preprocessing (Level 1B to Level 1C)

https://doi.org/10.5194/essd-2024-483
Preprint. Discussion started: 18 December 2024

Open Access Earth System Science Data Discussions

Figure 2 shows an example of POSP TOA Level 1B measurements on 2022-02-28 (Fig. 2a) and its corresponding Level 1C preprocessed for aerosol and surface retrieval (Fig. 2b). The TOA false color RGB image is composed with POSP reflectance from 670, 489 and 410 nm channels respectively.

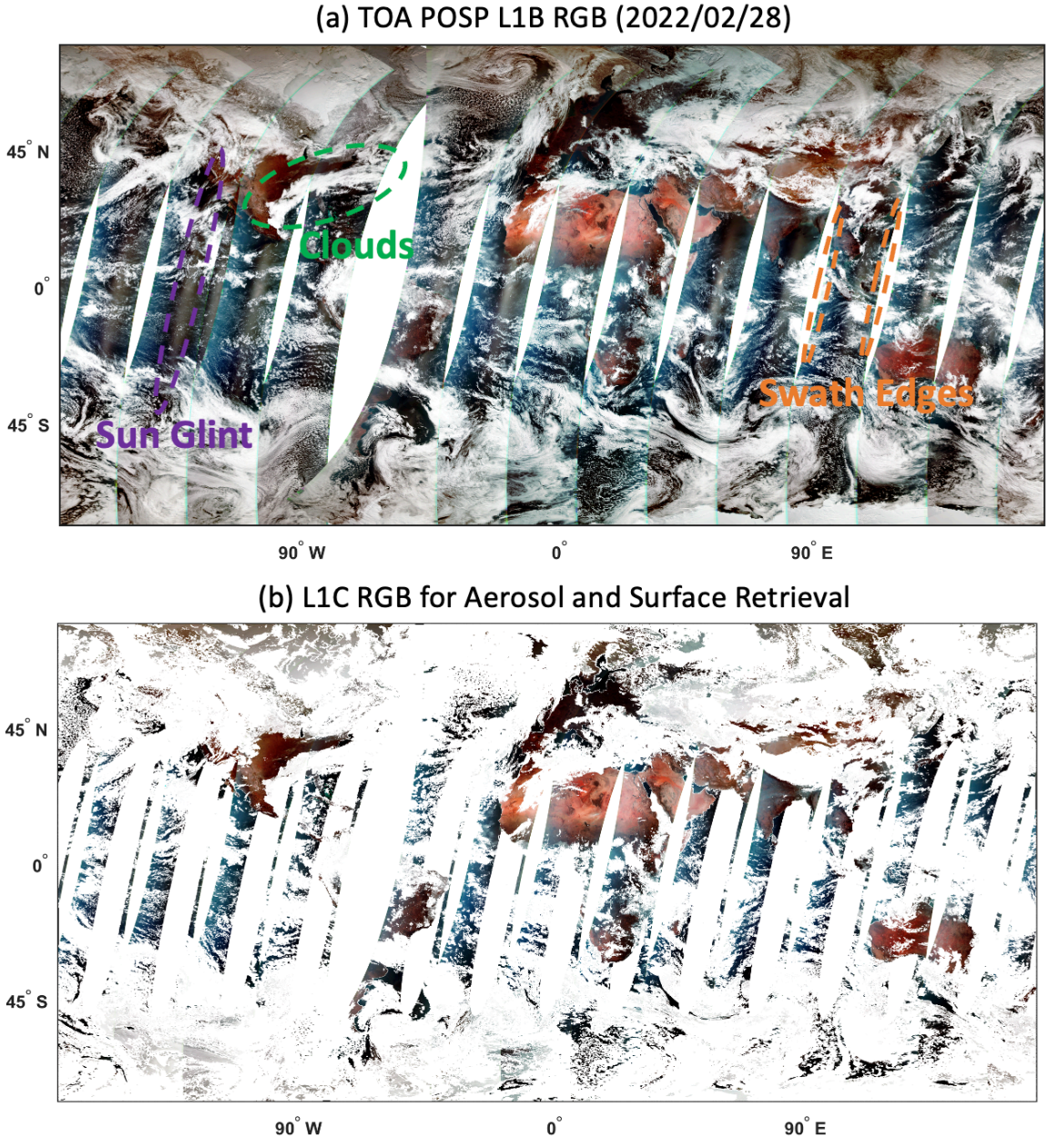

Figure 2. An example POSP TOA measurements on 2022-02-28 to illustrate (a) Level-1B TOA false color RGB and (b) Preprocessed Level-1C data prepared for aerosol and surface retrieval.

https://doi.org/10.5194/essd-2024-483
Preprint. Discussion started: 18 December 2024

155 **2.2 Datasets used for validation and evaluation**

2.2.1 Ground-based AERONET aerosol reference dataset

In order to validate the retrieval of aerosol optical and microphysical properties, the ground-based Aerosol Robotic Network (AERONET) aerosol reference dataset is used (Holben et al., 1998). AERONET direct-Sun multi-spectral aerosol optical depth (AOD), Ångström Exponent, spectral deconvolution algorithm (SDA) fine mode AOD (AODF) and coarse mode
160 AOD (AODC) (O'Neill et al., 2003), as well as single scattering albedo (SSA) from inversion product (Dubovik et al., 2000; Dubovik and King, 2000; Dubovik et al., 2000, 2002, 2006) are used to validate POSP aerosol retrievals. Specifically, we use the up-to-date AERONET Version 3 Level 2 products (last access: 2024-02-19) (Giles et al., 2019; Sinyuk et al., 2020; Smirnov et al., 2000) and make use of all AERONET sites with available data during the study period.

2.2.2 Space-borne aerosol and surface datasets from VIIRS and MODIS

165 Space-borne aerosol and surface datasets obtained from NOAA's Visible Infrared Imaging Radiometer Suite (VIIRS) aboard on the NOAA-20 satellite and NASA's Moderate Resolution Imaging Spectroradiometer (MODIS) aboard on the TERRA and AQUA satellites are used in this study to compare with derived POSP aerosol and surface products. Specifically, the NOAA20 VIIRS Deep Blue (DB) 6 km Level 2 aerosol product (AERDB_L2_VIIRS_NOAA20) is used to intercompare with the POSP aerosol product. The AERDB_L2_VIIRS_NOAA20 dataset includes spectral AOD at 412, 490, 550 and 670
170 nm over land and AOD at 490, 550 and 670 nm over ocean. The fine mode fraction at 550 nm is also provided over ocean that can be used to derive AODF and AODC at 550 nm (Hsu et al., 2019; Sayer et al., 2018a, b). For surface properties, the MODIS Collection 6.1 Albedo Model Parameters produced at 0.05° (degree) climate model grid datasets (MCD43C3) are used in the intercomparison including MCD43C3 surface albedos (white sky albedo and black sky albedo) at Band 1 (620-670 nm), Band 2 (841-876 nm), Band 3 (459-479 nm) and Band 7 (2105-2155 nm) (Schaaf and Wang, 2015).

175 **3 Aerosol and surface retrieval scheme and product specification**

3.1 POSP/GF-5(02) Level 2 aerosol and surface retrieval scheme

The GRASP/Models approach is used to retrieve aerosol and surface properties from POSP/GF-5(02) measurements. On the top of GRASP platform, several aerosol modeling approaches were developed by assuming different parameterization scheme for size distribution, complex refractive index, as well as chemical composition (Dubovik et al., 2011, 2021a; Li et
180 al., 2019; Chen et al., 2020). Among them, "Models" approach is one of the most simplified approaches with 6 spectral independent parameters to represent aerosol optical and microphysical properties. The GRASP/Models approach has been proven to be efficient to retrieve high-quality aerosol properties from different types of satellite remote sensing

https://doi.org/10.5194/essd-2024-483
Preprint. Discussion started: 18 December 2024

measurements, including multi-angular polarimeter, multi-spectral/hyperspectral spectrometer, etc. (Chen et al., 2020, 2022b, 2024a, b; Jin et al., 2022; Litvinov et al., 2024).

Specifically, aerosol total single scattering characteristics are assumed to be linear combination of the scattering characteristics of several pre-defined aerosol models (Eq. 2).

$$\omega(\lambda)\mathbf{P}(\lambda,\Theta) = \frac{\sum_{k=1}^{n} c_k C_{ext}^k(\lambda)\omega_k \mathbf{P}_k(\lambda,\Theta)}{\sum_{k=1}^{n} c_k C_{ext}^k(\lambda)} \quad (2)$$

Where λ indicates spectral channel; Θ is scattering angle; ω is aerosol single scattering albedo (SSA); $\mathbf{P}$ denotes phase matrix; k denotes one of n aerosol models; C_{ext} denotes total aerosol extinction; c_k denotes relative fraction for k-th aerosol model. Following previous applications on OLCI/Sentinel-3 and TROPOMI/Sentinel-5p (Chen et al., 2022b, 2024a; Litvinov et al., 2024), we use 4 models (n=4) approach to process POSP/GF-5(02), k=1 fine absorbing (biomass burning), k=2 fine slightly absorbing (urban/sulphate aerosol), k=3 coarse maritime (sea salt), k=4 coarse dust. The definition of 4 models' size distribution, spectral complex refractive index and non-sphericity are based on the AERONET climatology (Dubovik et al., 2002; Lopatin et al., 2021).

In addition, taking into account of the limited information from passive remote sensing measurements, aerosol microphysical properties are assumed to be identical at different vertical layers and only the total aerosol volume concentration and aerosol total extinction profile ($c_v = \tau_{ext}(\lambda)/\sum_{k=1}^{4} c_k C_{ext}^k(\lambda)$) varies following the exponential function.

$$c_v(z) = \frac{c_v}{h}\exp\left(-\frac{z}{h}\right) \quad (3)$$

Where z represents atmosphere vertical level; h is the aerosol layer height, namely scale height.

The sum of the semi-empirical Ross-Li sparse Bidirectional Reflectance Function (BRF) model (Li and Strahler, 1992; Roujean et al., 1992; Wanner et al., 1995) and the polarized reflection matrix R_p based on semi-empirical Maignan-Bréon BPDF (Bidirectional Polarization Distribution Function) models (Litvinov et al., 2010, 2011a, b; Maignan et al., 2009) are used to model surface reflectance for POSP/GF-5(02) processing. The kernel-driven Ross-Li BRDF model uses a linear combination of three kernels f_{iso}, f_{vol} and f_{geom} representing isotropic, volumetric and geometric optics surface scattering respectively (Li and Strahler, 1992; Roujean et al., 1992; Wanner et al., 1995). In addition, according to Litvinov et al. (Litvinov et al., 2010, 2011a, b), this model is further renormalized to spectral invariant of the second (a_{vol}) and third (a_{geom}) BRDF parameters in comparison to the first one $a_{iso}(\lambda)$. In GRASP, the polarized reflection matrix R_p is based on the semi-empirical Maignan-Bréon BPDF model (Maignan et al., 2009). For POSP/GF-5(02) processing, the wavelength independent scaling parameter (α) for Fresnel-based reflection matrix is retrieved.

https://doi.org/10.5194/essd-2024-483
Preprint. Discussion started: 18 December 2024

The ocean surface reflectance is modelled as combination of different ocean surface approaches. The Fresnel's reflection from the sea surface is taken into account using the Cox and Munk model (Cox and Munk, 1954). The water leaving radiance is assumed to be isotropic and is taken into account by Lambertian unpolarized reflectance (Voss et al., 2007). The relations between whitecaps/foam fraction and wind speed are defined by the empirical formula by Monahan and O'Muircheartaigh (1980). The spectral dependence of foam is accounted with the model described in (Frouin et al., 1996; Frouin and Pelletier, 2015). The detailed description of ocean surface reflectance modeling approach used in GRASP approach can be found in Litvinov et al. (2024) and Chen et al. (2022b). The spectral dependent isotropic water-leaving radiance $r_0(\lambda)$, Fresnel reflection fraction (free from foam, dense sediments, whitecaps etc.) δ_{Fr} and the mean square facet slope σ^2 are the directly retrieved parameters for ocean surface.

Then the state vector of each land and ocean pixel for POSP/GF-5(02) processing with GRASP/Models approach can be represented as follows:

$$\mathbf{X}^{land} = [c_v, c_1, c_2, c_3, c_4, h, a_{iso}(\lambda), a_{vol}, a_{geom}, \alpha]^T \quad (4)$$

$$\mathbf{X}^{ocean} = [c_v, c_1, c_2, c_3, c_4, h, r_0(\lambda), \delta_{Fr}, \sigma^2]^T \quad (5)$$

The inhomogeneous POSP 10 km pixels partially coved by water are skipped for the processing. Based on the directly retrieved parameters in state vector, aerosol optical-microphysical properties and surface properties, such as AOD, AODF, AODC, AAOD, SSA, NDVI, BRDF, BPDF, different surface albedos (White-Sky Albedo, Black-Sky Albedo) at UV, VIS, NIR and SWIR spectrum, can be calculated and delivered as a product.

The GRASP numerical inversion is implemented as a statistically optimized fitting of the observations using the least-square multi-Term principle (Dubovik et al., 2021a). GRASP implements a new multi-pixel technique to improve retrieval by simultaneously inverting large group of pixels (Dubovik et al., 2011, 2014). This approach allows for significant enhancement of atmosphere properties retrievals from remote sensing measurements by means of using additional a priori information about "correlation" retrieved properties in different pixels of the inverted group. The smallest processing group (segment) in the POSP/GRASP scheme is a group of 3x3xNT pixels, where NT is the number of measurements available in a month.

3.2 POSP/GF-5(02) Level 2 aerosol and surface products specification

The primary POSP/GF-5(02) aerosol product is the spectral AOD, which measures the column amount of aerosols in the atmosphere and is widely used in the community. POSP/GRASP Level 2 product offers spectral AOD at 9 wavelengths ranging from UV to SWIR. The product includes several additional aerosol characteristics such as AE, spectral fine/coarse mode AOD, spectral SSA and aerosol scale height. These specific aerosol characteristics are connected to aerosol particle size and absorption properties, which are important criteria for the aerosol climate and air quality community. The POSP/GRASP also offers full surface BRDF and BPDF characteristics, as well as the surface NDVI, spectral Directional

https://doi.org/10.5194/essd-2024-483
Preprint. Discussion started: 18 December 2024

Hemispherical Reflectance (DHR or black sky albedo) and spectral Surface Isotropic Bihemispherical Reflectance (BHR_{ISO} or white sky albedo). The POSP/GF-5(02) Level 2 aerosol and surface products are contained in a file typically named as: *GF5B_POSP_L2_Land_Ocean_{YYYYMMDD}.nc*. The product fields contained in the NetCDF-4 product file are listed in the Table 2.

Table 2. List of fields in the POSP/GF-5(02) Level 2 aerosol and surface product.

Variable Name	Dimension	LongName and Description
aaod{λ}	(y, x, λ)	Aerosol Absorption Optical Depth
AeroModelCon1	(y, x)	Aerosol fine absorbing mode fraction
AeroModelCon2	(y, x)	Aerosol fine non-absorbing mode fraction
AeroModelCon3	(y, x)	Aerosol oceanic mode fraction
AeroModelCon4	(y, x)	Aerosol dust mode fraction
AerosolConcentration	(y, x)	Aerosol total volume concentration
AExp	(y, x)	Ångström Exponent (442/865)
bhr_iso{λ}	(y, x, λ)	Surface Isotropic Bihemispherical Reflectance
dhr{λ}	(y, x, λ)	Directional Hemispherical Reflectance
land_percent	(y, x)	Percentage of land
LandBPDFMaignanBreon	(y, x)	Fresnel-based reflection matrix scaling parameter
LandBRDFRossLi{λ}_1	(y, x, λ)	Ross Li BRDF isotropic parameter
LandBRDFRossLi_2	(y, x)	Ross Li BRDF normalized volumetric parameter
LandBRDFRossLi_3	(y, x)	Ross Li BRDF normalized geometric parameter
lat	(y, x)	latitude
Lon	(y, x)	longitude
NDVI	(y, x)	Normalized Difference Vegetation Index
residual_absolute	(y, x)	Fitting Residual (absolute)
residual_relative	(y, x)	Fitting Residual (relative)
ssa{λ}	(y, x, λ)	Single Scattering Albedo
tau{λ}	(y, x, λ)	Aerosol Optical Depth
tauC{λ}	(y, x, λ)	Coarse mode Aerosol Optical Depth
tauF{λ}	(y, x, λ)	Fine mode Aerosol Optical Depth
unixtimestamp	(y, x)	Unix time in seconds from 1970/01/01T00:00:00 (UTC +8 hours)
VertProfileHeight	(y, x)	Scale height of vertical profile
WaterBRMCoxMunkIso{λ}_1	(y, x, λ)	Surface albedo of water body

https://doi.org/10.5194/essd-2024-483
Preprint. Discussion started: 18 December 2024

WaterBRMCoxMunkIso_2	(y, x)	Cox Munk BRDF fresnel fraction
WaterBRMCoxMunkIso_3	(y, x)	Cox Munk BRDF msq slope
X	x	WGS84 coordinates (easting)
Y	y	WGS84 coordinates (northing)

λ = 381, 410, 442, 489, 670, 865, 1611, 2254 nm

4 Preliminary validation and evaluation of POSP/GF-5B Level 2 product

4.1 Global distribution of POSP/GF-5(02) Level 2 aerosol and surface product

Based on the method proposed in Section 3, we processed first 18 months of POSP/GF-5(02) measurements from December 2021 to May 2023 using 4 intel 32-cores Think-Station. Figure 3 shows the spatial distribution of valid retrievals from December 2021 to May 2023. In summary, approximately 113 million pixels are retrieved successfully, account 70 million land pixels (~62%) and 43 million ocean pixels (~38%). Evidently, the ocean pixels percentage is much lower than expected, which can be associated with too strict cloud mask and glint mask used over ocean. This need to be adjusted and tested for future processing. We estimated the retrieval speed in order to constrain computational cost for future operational processing based on the18 months processing exercise. Approximately, for land pixels, the mean speed is 0.32 second / pixel / core with 1σ = 0.12 sec/pixel/core; for ocean pixels, the mean speed is 0.38 second / pixel / core with 1σ = 0.13 sec/pixel/core.

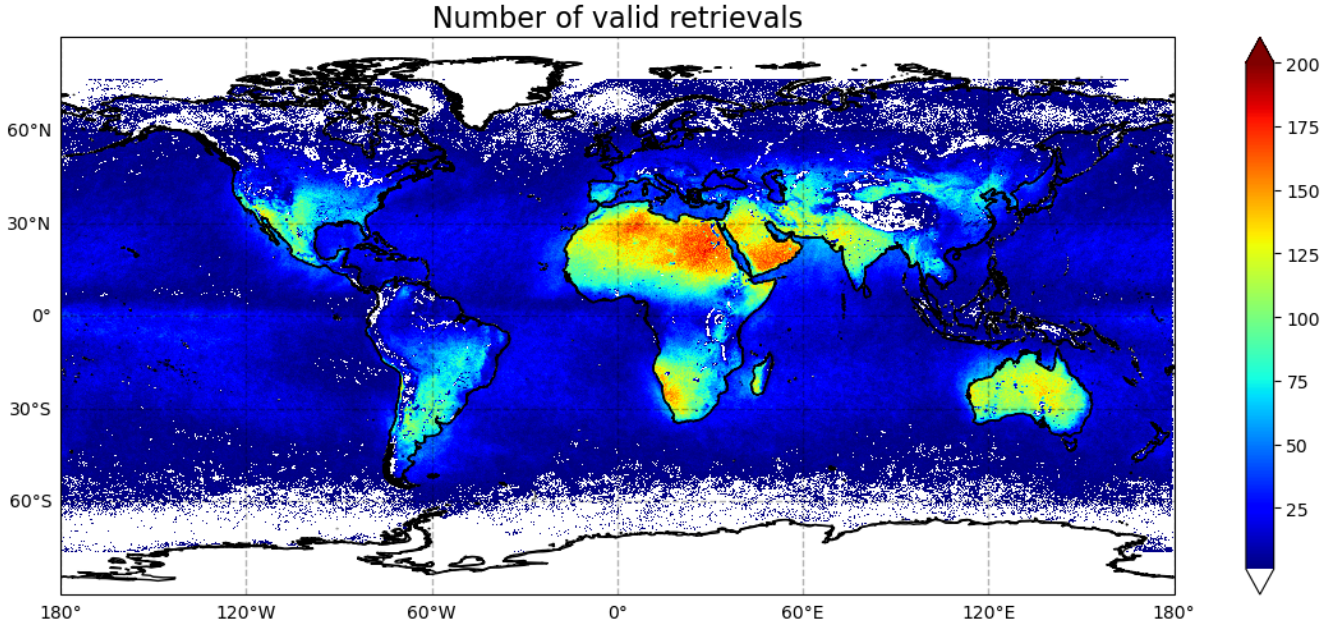

Figure 3. Spatial distribution of number of valid POSP/GRASP retrievals from December 2021 to May 2023.

https://doi.org/10.5194/essd-2024-483
Preprint. Discussion started: 18 December 2024

Open Access Earth System Science Data Discussions

In order to have a general picture of the POSP/GF-5(02) aerosol and surface product, we present the spatial distribution of POSP/GF-5(02) aerosol and surface main characteristics in Figure 4 (main aerosol products) and Figure 5 (main surface products) from December 2021 to May 2023. The main POSP/GF-5(02) aerosol products include spectral AOD, AODF, AODC and SSA range covering UV, VIS, NIR and SWIR spectrum, as well as AE (440/870), aerosol scale height (ALH). Note spectral aerosol absorption optical depth (AAOD) can be derived using $\mathrm{AAOD}(\lambda) = \mathrm{AOD}(\lambda) \times (1 - \mathrm{SSA}(\lambda))$ and is also provided in the product file. The main POSP/GF-5(02) surface products include full Ross Li BRDF parameters ($a_{iso}(\lambda), a_{vol}, a_{geom}$), Maignan-Bréon BPDF Fresnel-based reflection matrix scaling parameter (α), surface white sky albedo BHRiso(λ), black sky albedo DHR(λ), as well as surface Normalized Difference Vegetation Index (NDVI).

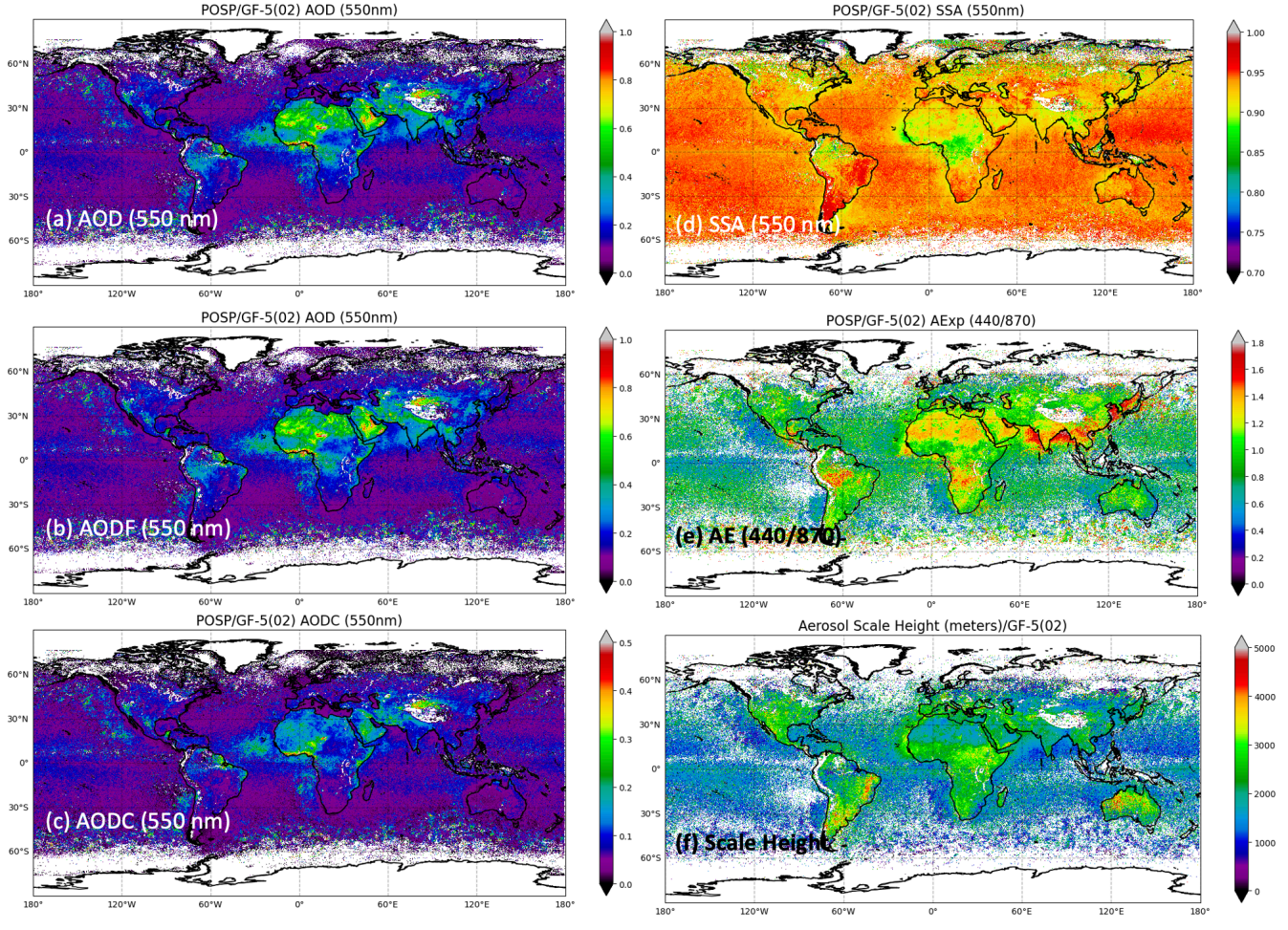

Figure 4. Spatial distribution of POSP/GF-5(02) main aerosol products: (a) Aerosol Optical Depth – AOD; (b) Fine mode Aerosol Optical Depth – AODF; (c) Coarse mode Aerosol Optical Depth (AODC); (d) Single Scattering Albedo – SSA; (e) Ångström Exponent – AE (440/870); (f) Scale height of aerosol vertical profile – ALH; Note AOD, AODF, AODC, SSA are spectral dependent and provided at UV, VIS, NIR and SWIR spectrum.

https://doi.org/10.5194/essd-2024-483
Preprint. Discussion started: 18 December 2024

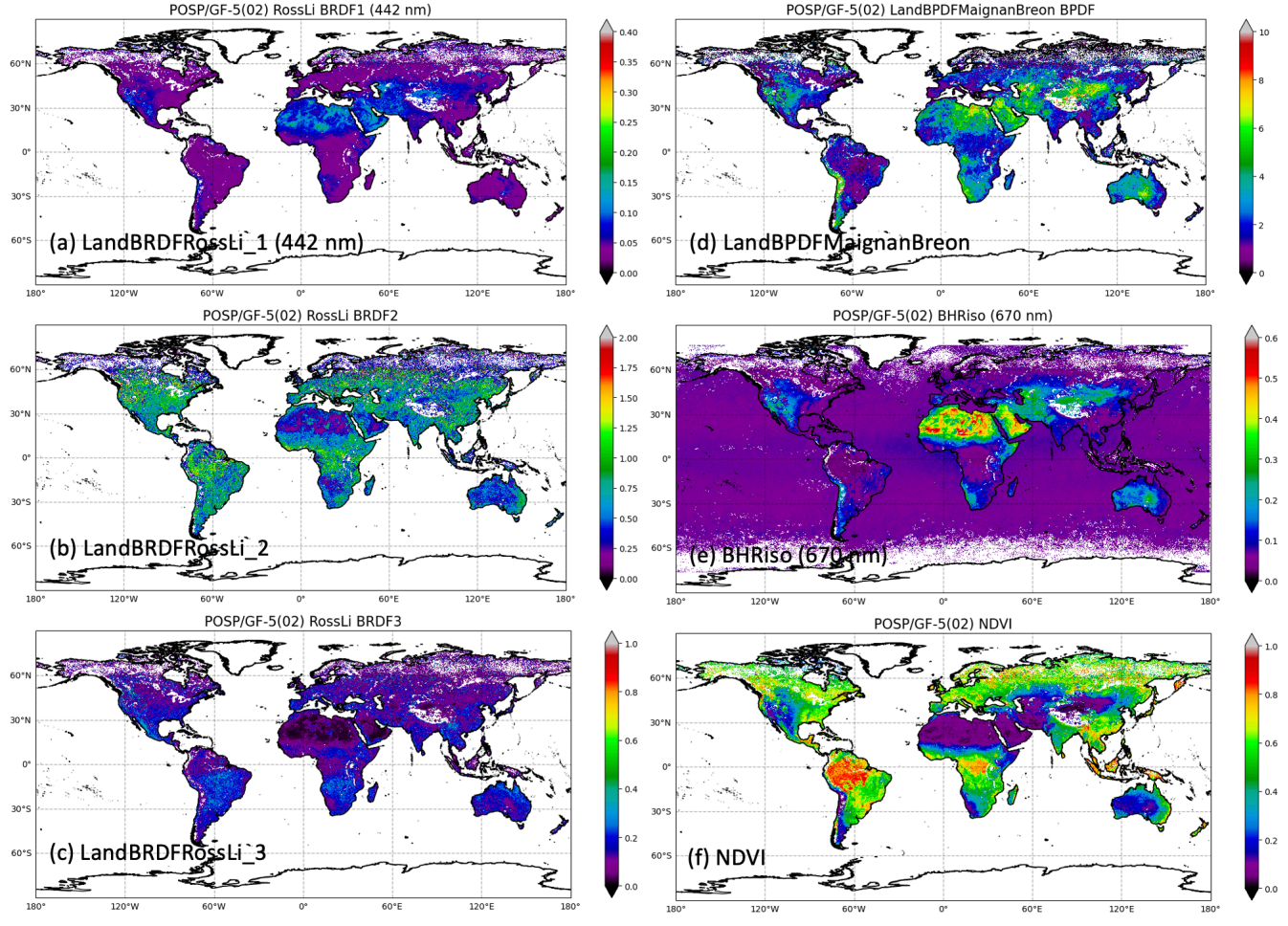

Figure 5. Spatial distribution of POSP/GF-5(02) main surface products: (a) Ross Li BRDF isotropic parameter; (b) Ross Li BRDF normalized volumetric parameter; (c) Ross Li BRDF normalized geometric parameter; (d) Maignan-Bréon BPDF; (e) Surface Isotropic Bihemispherical Reflectance – BHRiso or White Sky Albedo; (f) Normalized Difference Vegetation Index – NDVI. Note BRDF1 and BHRiso (White Sky Albedo) are spectral dependent and provided at UV, VIS, NIR and SWIR spectrum.

4.2 Validation of POSP/GF-5(02) aerosol product with AERONET

In order to verify the obtained spatial distribution of POSP aerosol and surface products, POSP aerosol product is validated with ground-based AERONET dataset. In order to match satellite retrievals with AERONET measurements, we follow the strategy used in our previous studies (Chen et al., 2020, 2022b, 2024a). Specifically, we use a 3 x 3 window centered over

https://doi.org/10.5194/essd-2024-483
Preprint. Discussion started: 18 December 2024

AERONET sites, and the satellite retrievals with a 3 x 3 window is averaged. Meanwhile, the available AERONET direct-Sun AOD, AE, AODF and AODC products are averaged within +/- 30 min of the POSP/GF-5(02) satellite overpass, and AERONET inversion SSA products are averaged within +/- 180 min of the POSP/GF-5(02) satellite overpass. For POSP, we have not yet introduced the quality flags into the product as for TROPOMI/Sentinel-5p (Litvinov et al., 2024). While, some experiences from TROPOMI/Sentinel-5p quality flag definition are used to select high-quality POSP retrievals for validation with AERONET. Basically, any retrieval meets the 3 conditions is defined as "high-quality" and will be used in validation.

(i) The relative fitting residual smaller than 5%;

(ii) Over land, the AOD (865 nm) standard deviation within its 3x3 window (STD_AOD_{865}) smaller than 0.1 or $STD\_AOD_{865} / \overline{AOD_{865}}$ smaller than 0.2, where $\overline{AOD_{865}}$ is the mean AOD with the 3x3 window. Over ocean, the STD_AOD_{865} is smaller than 0.05;

(iii) The number of valid retrievals with a 3x3 window need to be higher or equal to 3.

To quantify the validation results, several standard statistical parameters are used in this study, including linear correlation coefficient (R), the root mean square error (RMSE), the bias (BIAS), the fulfilment of the AOD Global Climate Observation System requirement (GCOS fraction), the formulated Target requirement for AOD, and the formulated Optimal and Target requirements for AE, SSA and surface albedos. Note the Optimal and Target requirements are formulated in our previous ESA S5P+I AOD/BRDF project (Litvinov et al., 2024) and were used in TROPOMI/Sentinel-5p validation (Chen et al., 2024a). Specifically, the GCOS requirement for AOD, AODF and AODC is max 0.04 or 10% (whatever is bigger); the Optimal requirements for AE, SSA and surface albedos are 0.3, 0.03 and 0.01 respectively; the Target requirement for AOD, AODF and AODC is max 0.05 or 20% (whatever is bigger), and the Target requirement for AE, SSA and surface albedos are 0.5, 0.05 and 0.02 respectively.

Figure 6 shows the validation of an entire year 2022 POSP/GF-5(02) GRASP AOD (550 nm) with AERONET over land (Fig. 6a) and ocean (Fig. 6c). Generally, POSP AOD (550 nm) show good agreement with AERONET both over land and ocean, with R=0.813, RMSE=0.114 over land and R=0.861, RMSE=0.091 over ocean. Moreover, the fulfilment of GCOS requirement is 47.6% over land and 54.3% over ocean. We intercompare the validation results obtained from TROPOMI/GRASP one year validation (Chen et al., 2024a; Litvinov et al., 2024). The obtained POSP validation statistical metrics are close to the TROPOMI validation results for QA>=2. Besides, the matchup points are evidently less than TROPOMI, which is associated with POSP's small swath width (1850 km) relative to TROPOMI (2600 km), and the scanning polarimeter has a large deformation at the edge of the track that we have to remove 10 pixels at the edge of the track.

https://doi.org/10.5194/essd-2024-483
Preprint. Discussion started: 18 December 2024

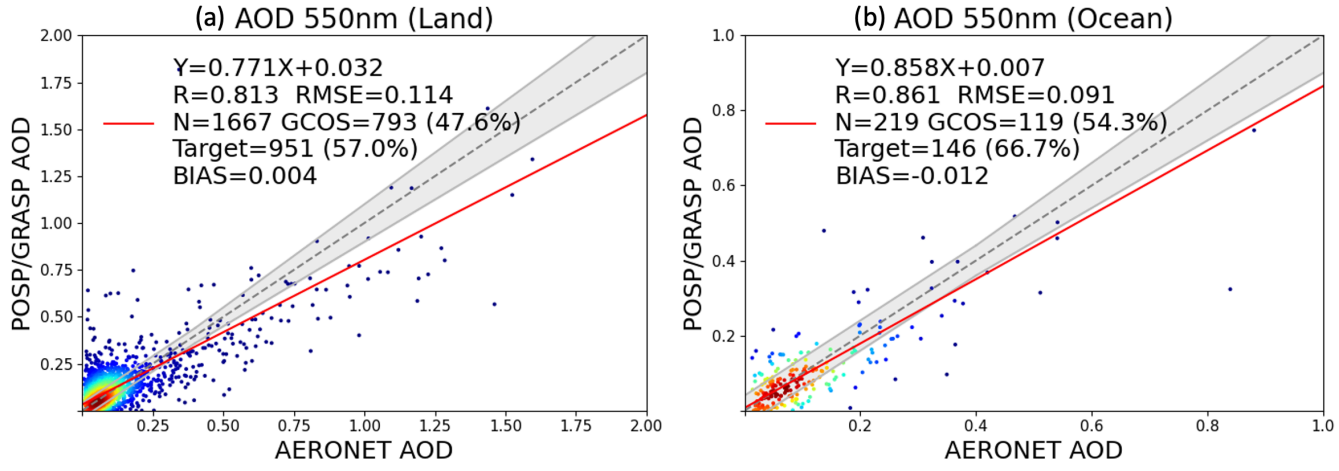

Figure 6. Validation of POSP/GF-5(02) GRASP AOD (550 nm) with AERONET over (a) land and (b) ocean for an entire year 2022.

The validation of POSP/GF-5(02) GRASP AE (440/870 nm) with AERONET is present in Figure 7 (7a – Land; 7b – Ocean). In order to ensure the quality of the satellite AE (440/870 nm) product, we usually filter low AOD cases for AE validation, due to the fact that the calculated AE is very sensitivity to the small variations in AOD at different wavelengths. For POSP AE validation, we select cases with POSP AOD (550 nm) > 0.2 over land and POSP AOD (550 nm) > 0.2 over ocean. Generally, POSP/GRASP tends to underestimate AE (too large particle size) for small particles (AE>1.0) and overestimate AE (too small particle size) for large particles (AE<1.0) over land. This is similar to the results obtained from OLCI and POLDER using GRASP/Models approach, and is associated with the particle size assumption for aerosol models. Moreover, the obtained AE>1.0 over Sahara Desert (Figure 4e) seems to be problematic, and is possibly related with polarimetric calibration or SWIR channel radiometric calibration that need further investigations. Over ocean, POSP/GRASP tends overestimate AE (too small particle size) for all ranges of AE. The results are consistent with the AODF and AODC validation presented in Figure 8 (AODF 550 nm) and Figure 9 (AODC 550 nm). Specifically, we observe a clear tendency over ocean that POSP/GRASP slightly overestimate fine mode AOD (Fig. 8b) while significantly underestimate coarse mode AOD (Fig. 9b). The validation of TROPOMI products show quiet similar feature (Chen et al., 2024a), which can be related with the fact that the space-borne downward measurements are more sensitive to suspended fine particles than coarse particles near the surface, while the ground-based upward measurements have much more sensitivity to coarse particles near the ground. This is our hypothesis that require more studies in the future.

https://doi.org/10.5194/essd-2024-483
Preprint. Discussion started: 18 December 2024

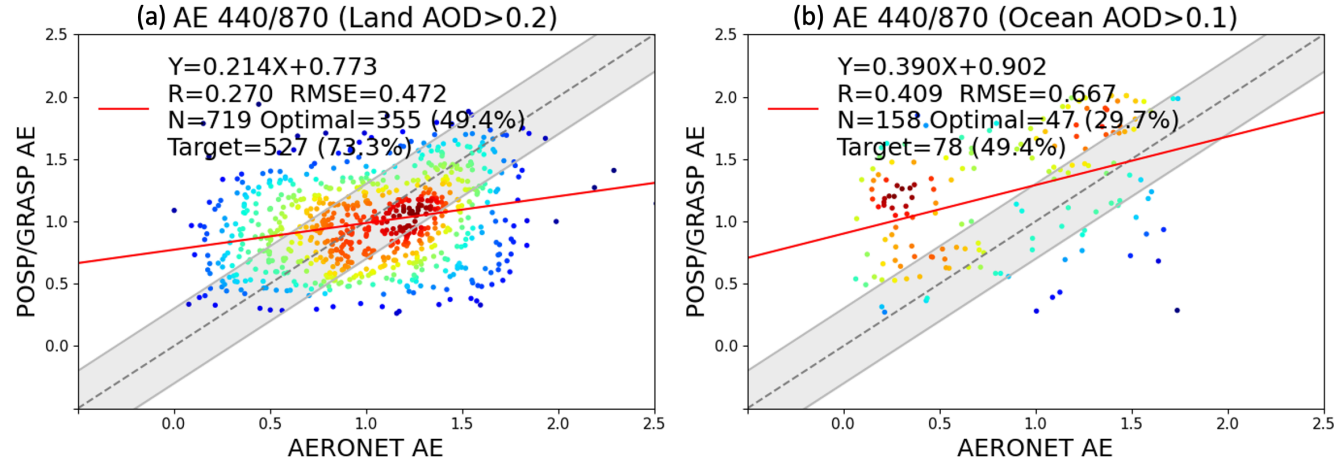

Figure 7. Validation of POSP/GF-5(02) GRASP AE (440/870) with AERONET over (a) land and (b) ocean for an entire year 2022.

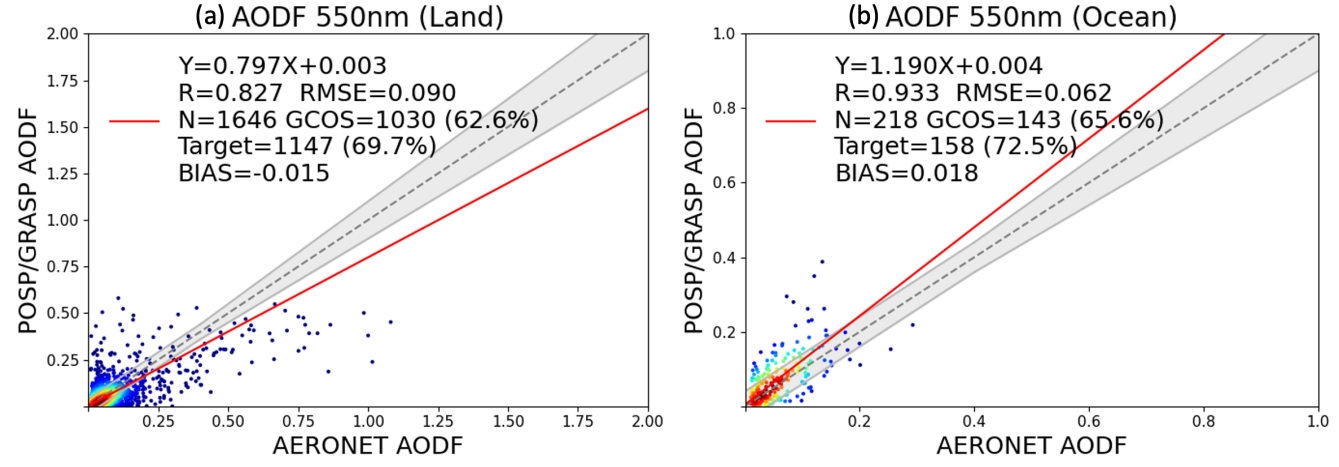

Figure 8. Validation of POSP/GF-5(02) GRASP AODF (550 nm) with AERONET over (a) land and (b) ocean for an entire year 2022.

https://doi.org/10.5194/essd-2024-483
Preprint. Discussion started: 18 December 2024

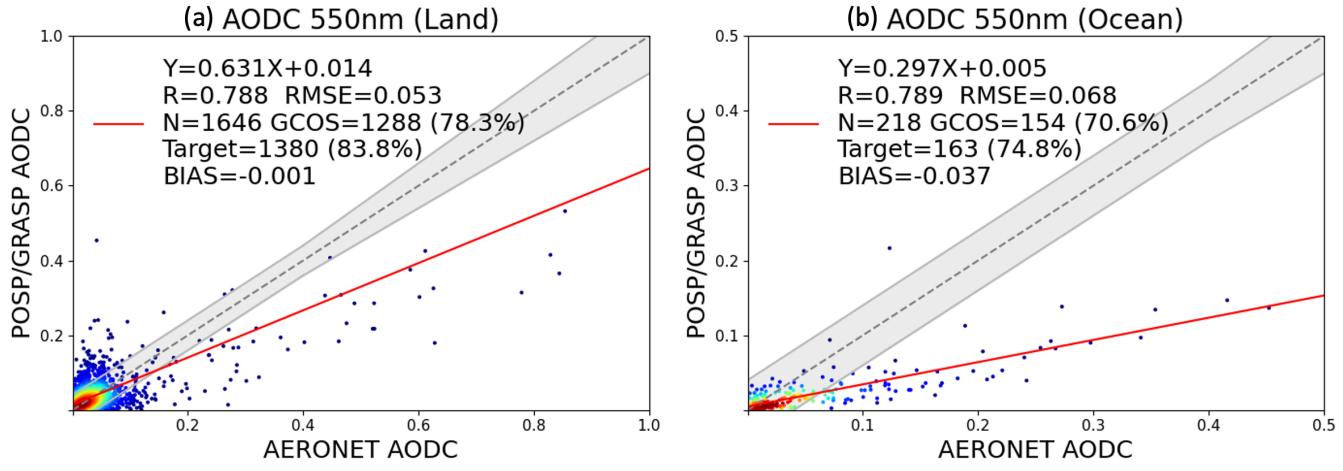

Figure 9. Validation of POSP/GF-5(02) GRASP AODC (550 nm) with AERONET over (a) land and (b) ocean for an entire year 2022.

In addition, we validate POSP/ POSP/GF-5(02) GRASP SSA (550 nm) with AERONET inversion products for an entire year 2022 and the results are shown in Figure 10. The AERONET Level 2 inversion SSA product is used as a reference where it contains aerosol loading filtering (AERONET AOD 440nm>0.4). For POSP/GRASP SSA, we also select the cases with POSP AOD (550 nm) > 0.2 to ensure the retrieval accuracy. POSP/GRASP SSA show good consistency with AERONET that RMSE is 0.040, BIAS is -0.007 and the fulfilment of SSA Optimal (+/- 0.03) and Target (+/- 0.05) requirements are 63.0% and 81.2% respectively.

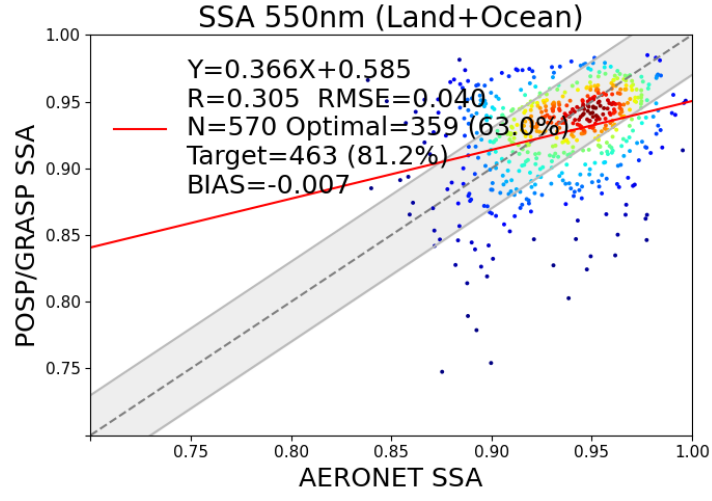

Figure 10. Validation of POSP/GF-5(02) GRASP SSA (550 nm) with AERONET over land and ocean for an entire year 2022.

https://doi.org/10.5194/essd-2024-483
Preprint. Discussion started: 18 December 2024

Overall, the performed AERONET validation results show that POSP/GF-5(02) GRASP aerosol product has good consistency with ground-based AERONET aerosol reference dataset, not only for AOD but also for detailed aerosol properties including AODF, AODC, AE as well as SSA. The validation results are basically comparable with previous aerosol products, such as OLCI/GRASP and TROPOMI/GRASP. This is a preliminary validation exercise for POSP aerosol product to obtain a general picture of the product quality and the instrument performance. In future, more in depth analysis of the product is certainly needed once more data is produced and the definition of the pixel-level quality flag is also in the to-do list for POSP product.

4.3 Intercomparison of POSP, MODIS and VIIRS aerosol and surface product

In this section, the POSP/GF-5(02) GRASP aerosol and surface product is intercompared with widely used NOAA and NASA aerosol and surface products, including NOAA-20 VIIRS DB aerosol product (AERDB_L2_VIIRS_NOAA20) and MCD43C3 surface white-sky-albedo. In order to compare the products at the same grid, we therefore re-grid POSP/GRASP 10 km, VIIRS/DB 6 km and MCD43C3 0.05° pixels onto common 0.2° x 0.2° grid box, and then the intercomparisons are performed for all 0.2° x 0.2° grid boxes globally. We still use similar criteria to select high quality retrievals for re-gridding. Specifically, for POSP/GF-5(02) product, we require the relative fitting residual smaller than 5% over land and ocean; for VIIRS/DB, we use the original retrievals with quality assurance QA>=2 over land and ocean.

Figure 11 shows the global spatial distribution of GF-5(02) POSP/GRASP (Fig. 11a) and NOAA-20 VIIRS/DB (Fig. 11b) AOD (550 nm) in 2022, as well as the pixel level difference of daily AOD (550 nm) averaged over entire year (Fig. 11c). On one hand, 2 products capture the global major aerosol features, such as Sahara dust, Taklimakan dust, southern Africa and southern America smoke, and high AOD over Indo-Gangetic Plain (IGP), etc. On the other hand, the 2 AOD products show non-neglectable differences in the AOD absolute values with spatial variability. For example, POSP/GRASP AOD (550 nm) is generally 0.05-0.15 higher than VIIRS/DB over desert region (Sahara, Taklimakan and Arabian Peninsula), and POSP/GRASP AOD (550 nm) is slightly 0.03-0.10 lower than VIIRS/DB over central and southern Africa biomass burning region and India region. Statistically, the one-year global all grid boxes AOD (550 nm) metrics between POSP/GRASP and VIIRS/DB are presented in Figure 12. Based on ~10 million matchup grid boxes (5.3 million over land and 4.4 million over ocean), the grid-to-grid AOD (550 nm) linear correlation coefficients (R) between POSP/GRASP and VIIRS/DB are 0.675 over land and 0.746 over ocean, with differences (POSP-VIIRS) +0.043 (1σ=0.182) over land and -0.029 (1σ=0.074) over ocean. Generally, the AOD intercomparison results are reasonable while not as good as our previous exercise for TROPOMI/Sentinel-5p vs. VIIRS/SNPP (Chen et al., 2024a). One intrinsic reason is the difference of satellite overpass time are few hours between GF-5(02) and NOAA-20 in contrast with few minutes between Sentinel-5p and SNPP. Besides, there are some potential reasons need to verify in the future, for example, the data quality, calibration accuracy, cloud mask, etc.

https://doi.org/10.5194/essd-2024-483
Preprint. Discussion started: 18 December 2024

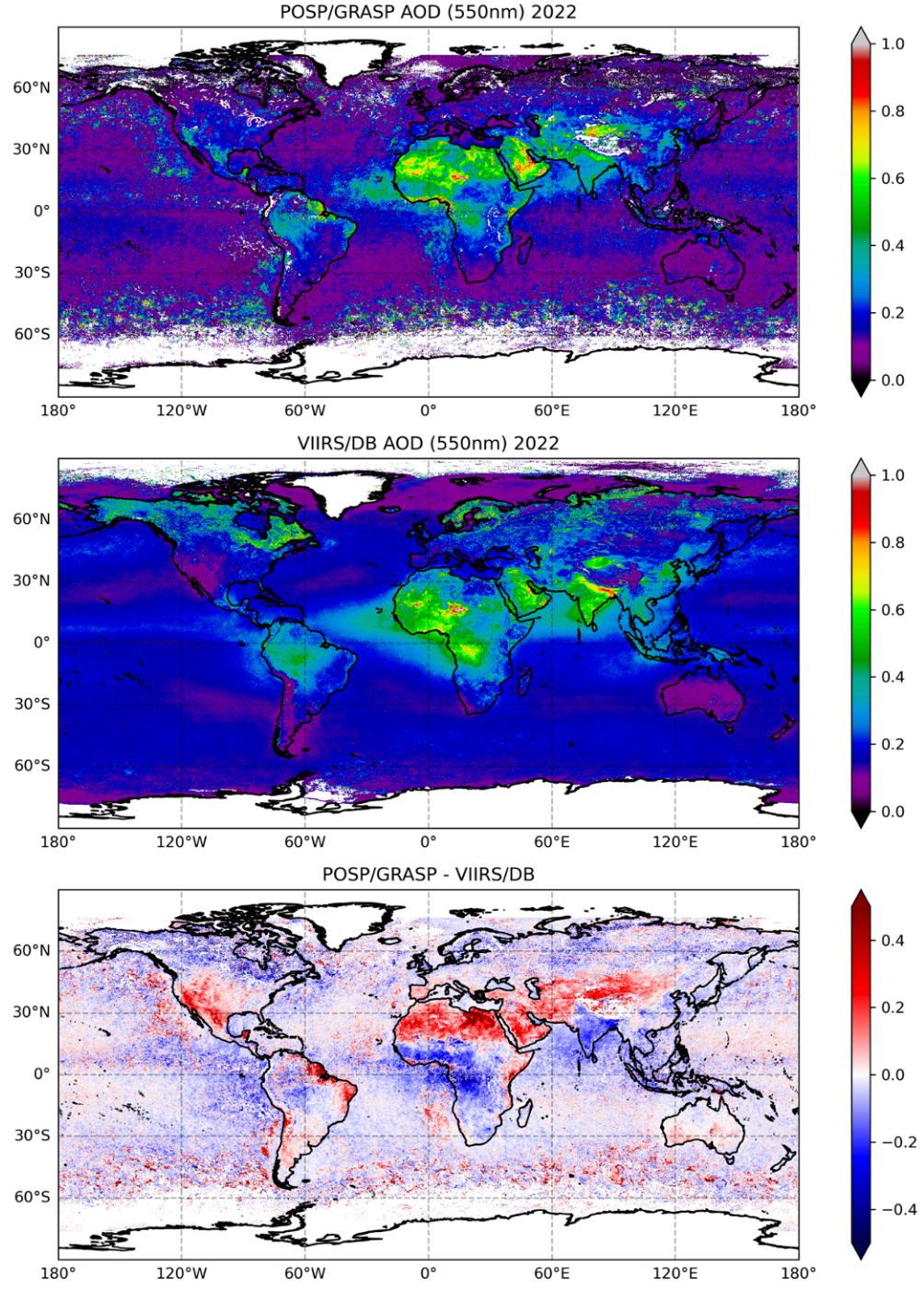

Figure 11. Spatial distribution of one-year (2022) AOD (550 nm) from GF-5(02) POSP/GRASP and NOAA-20 VIIRS/DB. The pixel level difference of AOD 550 nm averaged over a year is presented at the bottom as POSP/GRASP - VIIRS/DB.

https://doi.org/10.5194/essd-2024-483
Preprint. Discussion started: 18 December 2024

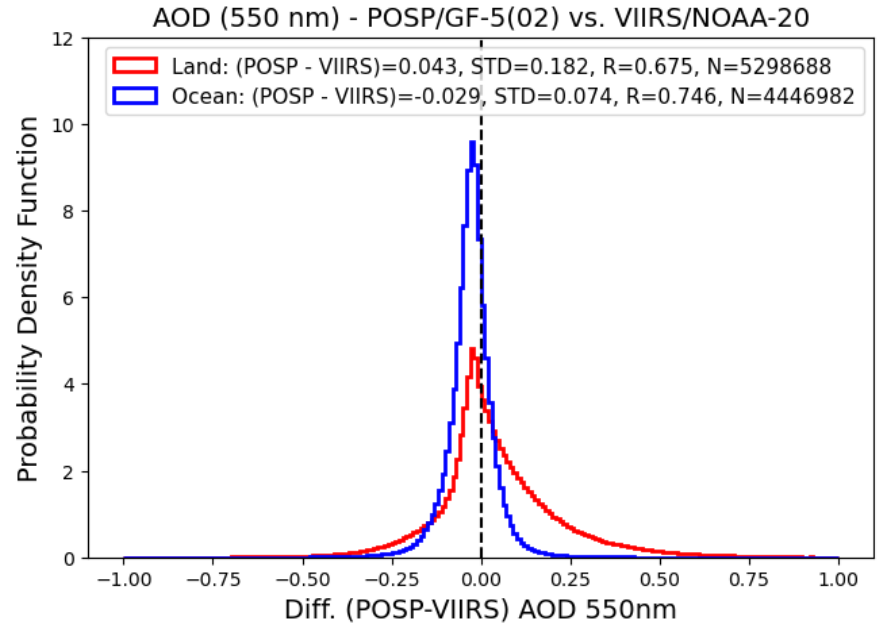

Figure 12. Possibility density function (PDF) of global all 0.2° x 0.2° grid box AOD (550 nm) differences between VIIRS/DB and POSP/GRASP over land and ocean.

Figure 13 shows the global spatial distribution of GF-5(02) POSP/GRASP and NOAA-20 VIIRS/DB AODF (550 nm) and AODC (550 nm) in 2022, as well as the pixel level difference of daily AODF and AODC averaged over entire year. Note that the VIIRS/DB fine mode fraction (FMF) is only available over ocean provide by Satellite Ocean Aerosol Retrieval (SOAR) algorithm (Sayer et al., 2018a, 2018b). The intercomparison of AODF and AODC are performed over ocean only. The one-year global all grid boxes AODF (550 nm) and AODC (550 nm) metrics between POSP/GRASP and VIIRS/DB are presented in Figure 14. Some clear tendencies are identified for AODF and AODC over ocean. Specifically, POSP/GRASP AODF (550 nm) is almost everywhere 0.01 higher than VIIRS/DB, while POSP/GRASP AODC (550 nm) is generally 0.02-0.05 lower than VIIRS/DB. These results are also seen by AERONET validation that POSP seems to overestimate AODF while underestimate AODC over ocean (Figs. 8b and 9b), as well as the AE validation (Fig. 7b) that POSP seems to underestimate particle size (overestimate AE) over ocean. This is potentially associate with the coarse models (dust and oceanic maritime) used in GRASP/Models. Overall, the agreement between 2 satellites AOD, AODF and AODC products generated with 2 independent algorithms are generally reasonable with R around 0.7-0.75, RMSE around 0.18 over land and 0.08 over ocean for total AOD, and RMSE around 0.05 for AODF and AODC over ocean.

https://doi.org/10.5194/essd-2024-483
Preprint. Discussion started: 18 December 2024

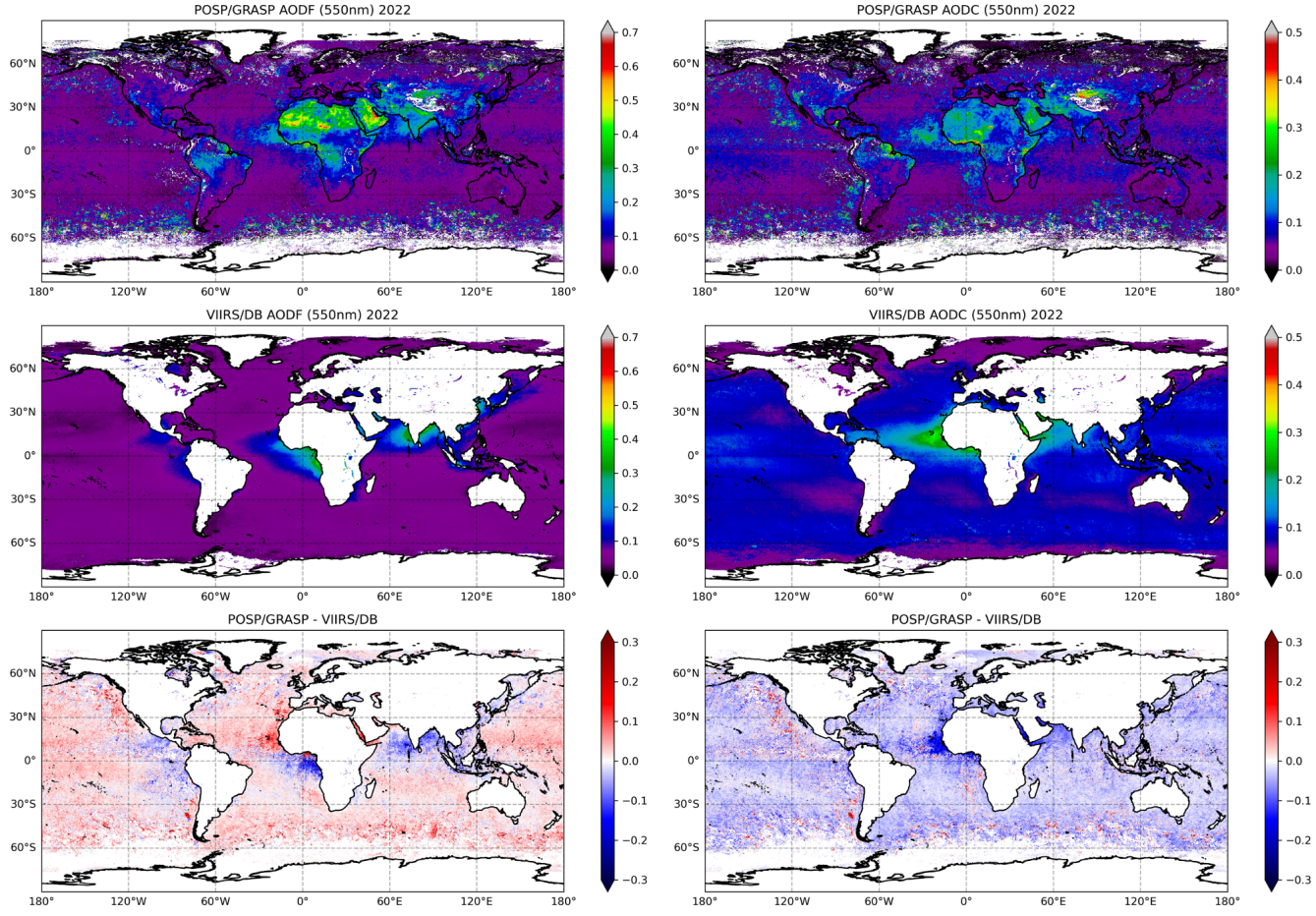

Figure 13. Spatial distribution of one-year (2022) left column: AODF (550 nm) and right column: AODC (550 nm) from GF-5(02) POSP/GRASP and NOAA-20 VIIRS/DB. The pixel level difference of AODF and AODC at 550 nm averaged over a year is presented at the bottom as POSP/GRASP - VIIRS/DB.

425

https://doi.org/10.5194/essd-2024-483
Preprint. Discussion started: 18 December 2024

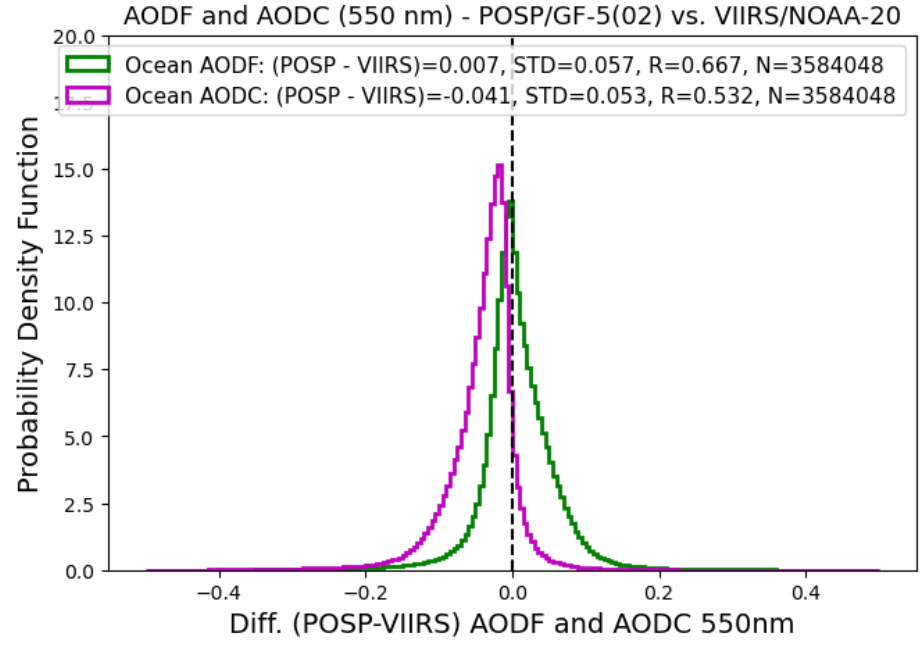

Figure 14. Possibility density function (PDF) of global all 0.2° x 0.2° grid box AODF (550 nm) and AODC (550 nm) differences between VIIRS/DB and POSP/GRASP over ocean.

For surface product, we intercompare POSP/GF-5(02) GRASP and MODIS MCD43C3 surface white-sky-albedos at blue (442 nm vs. MODIS Band3), red (670 nm vs. MODIS Band1), NIR (865 nm vs. MODIS Band2) and SWIR (2254 nm vs. MODIS Band7) channels. The intercomparison strategy is the same as our previous study (Chen et al., 2022b, 2024a) that all global 0.2° x 0.2° grid box intercomparison is performed using monthly means. We should note that the MODIS MCD43C3 product is accumulation of 16-days TERRA and AQUA data and weighted to the day of interest, therefore we use the data on the 15th day of each month to approximate the MODIS monthly mean surface albedos. In addition, the differences of the channel center wavelength and the bandwidth are different between POSP and MODIS. Therefore, the objective of the intercomparison exercise is to get a general idea of the 2 surface albedo products and analysis some trends that may be related to instrument performance.

Figure 15 shows the spatial distribution of one-year POSP/GF-5(02) and MODIS MCD43C3 BHRiso (white sky albedo) at blue, red, NIR and SWIR channels. Statistically, the one-year global all grid boxes BHRiso metrics between POSP/GRASP and MODIS MCD43 are presented in Figure 16a, together with the monthly variation of the white-sky-albedo differences between POSP and MODIS in 2022 in Figure 16b (visible channels) and Figure 16c (NIR and SWIR channels). The surface Optimal (+/-0.01) and Target (+/-0.02) requirements used in this study are formulated in ESA S5P+I AOD/BRDF project (Litvinov et al., 2024). Because surface is the dominant TOA signal in general, we observe quite consistent global spatial

https://doi.org/10.5194/essd-2024-483
Preprint. Discussion started: 18 December 2024

variability between POSP and MODIS BHRiso at blue, red, NIR and SWIR channels. The best agreement between 2 products is observed at two visible channels (blue and red), especially at 670 nm. The global differences (POSP-MODIS) are around 0.002-0.003 with 1σ variation about 0.023, and the fulfillment of Target and Optimal requirements are ~75% and ~50% respectively. While, the differences become large at NIR (-0.022, 1σ=0.038) and SWIR (-0.046, 1σ=0.057) channels. In addition, the SWIR channel difference is even larger (around -0.08 ~ -0.1) over Sahara and other desert regions, which is potentially connected with the overestimation of fine mode particles over desert regions (Fig. 4b and 4e). Certainly, we must acknowledge the difference of two channels (POSP 2254 nm vs. MODIS 2105-2155 nm). Taking into account the new instrument POSP and the general challenges with the calibration of SWIR channels, we infer that the calibration of POSP SWIR channels may underestimate high values. This is an inference from intercomparison analysis of indirect surface albedos that need further verification with Level 1 calibration team.

Discussions
Earth System Science Data
Open Access

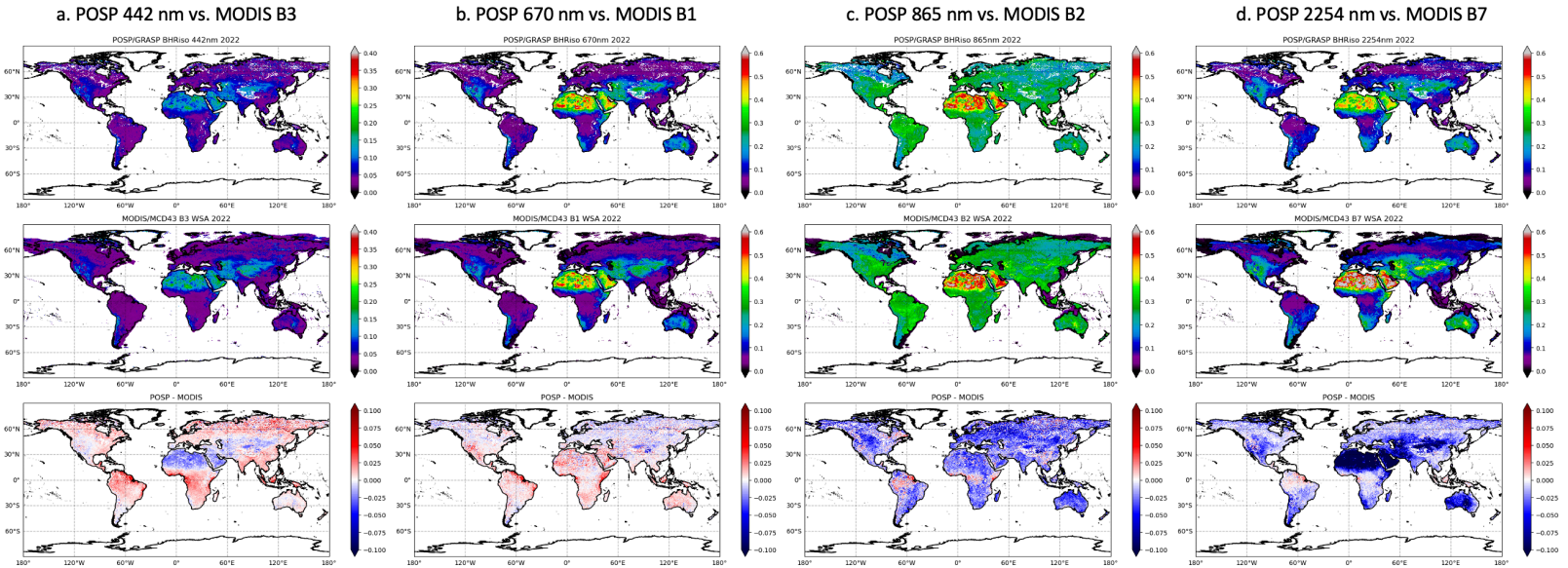

Figure 15. Spatial distribution of one-year (2022) POSP/GF-5(02) and MODIS MCD43 BHRiso (white sky albedo) at blue, red, NIR and SWIR channels. (a) POSP 442 nm vs. MODIS B3 459-479 nm; (b) POSP 670 nm vs. MODIS B1 620-670 nm; (c) POSP 865 nm vs. MODIS B2 841-876 nm; (d) POSP 2254 nm vs. MODS B7 2105-2155 nm. The pixel level difference averaged over a year is presented at the bottom as POSP/GRASP - VIIRS/DB.

https://doi.org/10.5194/essd-2024-483
Preprint. Discussion started: 18 December 2024

https://doi.org/10.5194/essd-2024-483
Preprint. Discussion started: 18 December 2024

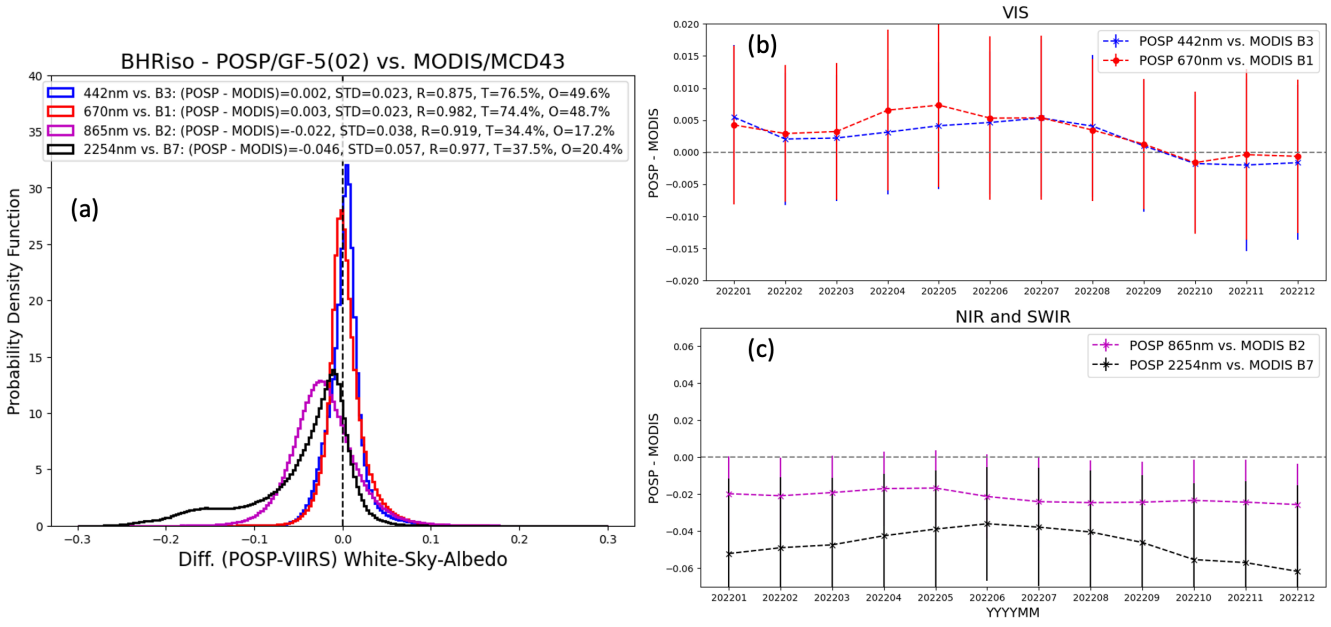

Figure 16. (a) Possibility density function (PDF) of global all 0.2° x 0.2° grid box white sky albedo differences between MODIS/MCD43 and POSP/GRASP. Monthly variation of the white-sky albedo differences between POSP and MODIS in 2022: (b) visible channels; (c) NIR and SWIR channels. The error bar indicates the 1σ variation of the differences (POSP-MODIS).

5 Summary and conclusions

In this study, we provide a detailed description of the development of aerosol and surface Level 2 product and the processing scheme for the first space-borne UV-VIS-NIR-SWIR multi-spectral cross-track scanning polarimeter (POSP) onboard Chinese GF-5(02) satellite based on the GRASP/Models approach. Since POSP is a new polarimeter collecting both intensity and polarimetric measurements at UV, VIS, NIR and SWIR channels, we intend to verify the performance and feasibility of the instrument through the development of aerosol and surface products, validation and intercomparison with reference datasets and other independent satellite products. The total 18 months of POSP/GF-5(02) measurements from December 2021 to May 2023 were processed, and the obtained global aerosol and surface properties are evaluated and delivered as the baseline POSP product. We will continue to processing the data and deliver up-to date POSP/GF-5(02) aerosol and surface products.

https://doi.org/10.5194/essd-2024-483
Preprint. Discussion started: 18 December 2024

Generally, we found the POSP single-viewing, multi-spectral (UV-VIS-NIR-SWIR) polarimetric measurements provide rich information content for aerosol and surface characterization, not only total aerosol optical depth, but also detailed properties including aerosol size, absorption, layer height, type, etc. We provide spectral AOD, AODF, AODC, AE and SSA ranging from UV to SWIR, as well as aerosol scale height, columnar volume concentration for 4 aerosol models (BB – BC and OC/BC, Urban - sulfate, Oceanic – sea salt and dust) in the POSP/GF-5(02) aerosol product, and full BRDF, BPDF parameters, derived black-sky/white-sky albedos and vegetation index NDVI in the POSP/GF-5(02) surface product.

The validation of POSP one entire year (2022) aerosol product with ground-based AERONET reference data show general good agreement. Specifically, the correlation coefficients R for AOD (550 nm) are around 0.82-0.87 over land and ocean, and RMSEs are within 0.12 over land and ~0.09 over ocean. The fulfilment of AOD GCOS requirement is around 48% and 55% over land and ocean respectively. For aerosol particle size related parameters (AODF, AODC and AE), POSP AODF (550 nm) show good consistency with AERONET SDA product with R around 0.8 both over land and ocean, and bias is within 0.015. POSP AODC (550 nm) has good correlation coefficient with AERONET that R is 0.93 over land and 0.79 over ocean, while POSP tends to overestimate (0.02) AODC over land and underestimate AODC (0.03-0.04) over ocean. Similarly, the validation of POSP AE indicates that POSP tends to underestimate particle size (overestimate AE) over ocean, and this tendency is also observed over bright land surface, especially over desert regions where POSP tends to overestimate AE and fine mode AOD.

The POSP/GF-5(02) aerosol and surface products are then intercompared with VIIRS/NOAA-20 DB aerosol and MODIS MCD43 surface products globally at common 0.2° x 0.2° grid box. Based on around 10 million grid box intercomparison, POSP/GRASP and VIIRS/DB total AOD (550 nm) show reasonable agreement with R around 0.7-0.75, RMSE around 0.18 over land and 0.08 over ocean, and POSP global mean AOD (550 nm) is about 0.04 higher than VIIRS over land and 0.03 smaller than VIIRS over ocean. Over land, POSP tends to report higher AOD than VIIRS over desert regions, where POSP seems to always overestimate fine mode contribution. This phenomenon can be associated with the POSP polarimetric calibration or SWIR channel radiometric calibration. For AODF and AODC over ocean, POSP/GRASP generally report higher AODF and lower AODC than VIIRS/DB. This also can be connected with POSP radiometric calibration and the coarse mode assumptions used in GRASP/Models approach. The intercomparison POSP/GRASP and MODIS MCD43 surface white-sky-albedos show overall good consistency in VIS channels (blue and red), while POSP tends to report smaller white-sky-albedos at NIR (-0.02) and SWIR (-0.045) channels than that from MODIS which is possibly due to the signal attenuation that require recalibration.

In the past, for Chinese satellite missions, ground segment is somehow insufficiently regarded as it should be. Here, some lessons are learnt during the development of the global aerosol and surface products from POSP onboard GF-5(02) satellite. (i) Some useful and important pixel level identification or classification are missing or need to improve in Level 1 data. For

https://doi.org/10.5194/essd-2024-483
Preprint. Discussion started: 18 December 2024

example, cloud mask is not well documented and functional well. We would recommend to include additional surface identifications, such as coastal line, mixed land and water, snow, ice, saline lake etc. and auxiliary data potential from reanalysis dataset, such as gas concentration, wind speed, etc., which are very helpful to develop high-quality Level 2 product. (ii) On-orbit calibration requires continuous efforts and consistent iteration with proper versioning of the product. Overall, the POSP/GF-5(02) baseline aerosol and surface Level 2 product is developed and will continue processing and release the product that verified the good performance of the first space-borne multi-spectral cross-track scanning polarimeter (POSP).

Data availability

The developed POSP/GF-5(02) aerosol and surface products are publicly available and registered at doi.org/10.57760/sciencedb.14748 (Chen et al., 2024c).

Author contribution

C. C., Z. Q. L. and J. H. convinced the initial idea for the study. X. L., Z. H. L., G. X., M. B. and Z. Q. support for the Level 1 data preparation and Level 2 data processing resources. C. C., O. D., P. L., D. F. developed and supported for the retrieval scheme. C. C., Z. Q. L., X. L. and H. G. performed the retrieval tests and carried out the processing. C.C. and Z. Q. L. wrote the manuscript with comments from all the authors.

Competing interests

The authors declare that they have no conflict of interest.

References

Bréon, F.-M., Vermeulen, A., and Descloitres, J.: An evaluation of satellite aerosol products against sunphotometer measurements, Remote Sens Environ, 115, 3102–3111, https://doi.org/10.1016/J.RSE.2011.06.017, 2011.

Cairns, B., Waquet, F., Knobelspiesse, K., Chowdhary, J., and Deuzé, J.-L.: Polarimetric remote sensing of aerosols over land surfaces, Satellite Aerosol Remote Sensing over Land, 295–325, https://doi.org/10.1007/978-3-540-69397-0_10, 2009.

Chen, C., Dubovik, O., Fuertes, D., Litvinov, P., Lapyonok, T., Lopatin, A., Ducos, F., Derimian, Y., Herman, M., Tanré, D., Remer, L., Lyapustin, A., Sayer, A., Levy, R., Hsu, N. C., Descloitres, J., Li, L., Torres, B., Karol, Y., Herrera, M., Herreras, M., Aspetsberger, M., Wanzenboeck, M., Bindreiter, L., Marth, D., Hangler, A., and Federspiel, C.:

https://doi.org/10.5194/essd-2024-483
Preprint. Discussion started: 18 December 2024

Validation of GRASP algorithm product from POLDER/PARASOL data and assessment of multi-angular polarimetry potential for aerosol monitoring, Earth Syst Sci Data, 12, 3573–3620, https://doi.org/10.5194/essd-12-3573-2020, 2020.

Chen, C., Dubovik, O., Schuster, G. L., Chin, M., Henze, D. K., Lapyonok, T., Li, Z., Derimian, Y., and Zhang, Y.: Multi-angular polarimetric remote sensing to pinpoint global aerosol absorption and direct radiative forcing, Nature Communications 2022 13:1, 13, 1–11, https://doi.org/10.1038/s41467-022-35147-y, 2022a.

Chen, C., Dubovik, O., Litvinov, P., Fuertes, D., Lopatin, A., Lapyonok, T., Matar, C., Karol, Y., Fischer, J., Preusker, R., Hangler, A., Aspetsberger, M., Bindreiter, L., Marth, D., Chimot, J., Fougnie, B., Marbach, T., and Bojkov, B.: Properties of aerosol and surface derived from OLCI / Sentinel-3A using GRASP approach : Retrieval development and preliminary validation, Remote Sens Environ, 280, 113142, https://doi.org/10.1016/j.rse.2022.113142, 2022b.

Chen, C., Litvinov, P., Dubovik, O., Bindreiter, L., Matar, C., Fuertes, D., Lopatin, A., Lapyonok, T., Lanzinger, V., Hangler, A., Aspetsberger, M., de Graaf, M., Tilstra, L. G., Stammes, P., Dandocsi, A., Gasbarra, D., Fluck, E., Zehner, C., and Retscher, C.: Extended aerosol and surface characterization from S5P/TROPOMI with GRASP algorithm. Part II: Global validation and Intercomparison, Remote Sens Environ, 313, 114374, https://doi.org/10.1016/J.RSE.2024.114374, 2024a.

Chen, C., Litvinov, P., Dubovik, O., Fuertes, D., Matar, C., Miglietta, F., Pepe, M., Genesio, L., Busetto, L., Bindreiter, L., Lanzinger, V., de Graaf, M., Tilstra, G., Stammes, P., and Retscher, C.: Retrieval of Aerosol and Surface Properties at High Spatial Resolution: Hybrid Approach and Demonstration Using Sentinel-5p/TROPOMI and PRISMA, Journal of Geophysical Research: Atmospheres, 129, e2024JD041041, https://doi.org/10.1029/2024JD041041, 2024b.

Chen, C., Lei, X., Liu, Z., Gu, H., Hong, J., Li, Z.: Aerosol and surface products from cross-track scanning polarimeter POSP onboard GF-5(02) satellite (December 2021 - May 2023) [DS/OL]. V1. Science Data Bank, 2024 [2024-10-21]. https://cstr.cn/31253.11.sciencedb.14748. CSTR:31253.11.sciencedb.14748, 2024c.

Chen, F., Luo, D., Li, S., Yang, B., Sun, L., Ge, S., and Hong, J.: The Operational Inflight Radiometric Uniform Calibration of a Directional Polarimetric Camera, Remote Sensing 2021, Vol. 13, Page 3823, 13, 3823, https://doi.org/10.3390/RS13193823, 2021a.

Chen, L., Shang, H., Fan, M., Tao, J., Husi, L., Zhang, Y., Wang, H., Cheng, L., Zhang, X., Wei, L., Li, M., Zou, M., and Liu, D.: Mission overview of the GF-5 satellite for atmospheric parameter monitoring, National Remote Sensing Bulletin, 25, 1917–1931, https://doi.org/10.11834/JRS.20210582/, 2021b.

Chen, L., Letu, H., Fan, M., Shang, H., Tao, J., Wu, L., Zhang, Y., Yu, C., Gu, J., Zhang, N., Hong, J., Wang, Z., and Zhang, T.: An Introduction to the Chinese High-Resolution Earth Observation System: Gaofen-1~7 Civilian Satellites, Journal of Remote Sensing, 2022, https://doi.org/10.34133/2022/9769536, 2022c.

Cox, C. and Munk, W.: Measurement of the Roughness of the Sea Surface from Photographs of the Sun's Glitter, J Opt Soc Am, 44, 838, https://doi.org/10.1364/josa.44.000838, 1954.

Deschamps, P.-Y., Breon, F.-M., Leroy, M., Podaire, A., Bricaud, A., Buriez, J.-C., and Seze, G.: The POLDER mission:

instrument characteristics and scientific objectives, IEEE Transactions on Geoscience and Remote Sensing, 32, 598–615, https://doi.org/10.1109/36.297978, 1994.

Dubovik, O. and King, M. D.: A flexible inversion algorithm for retrieval of aerosol optical properties from Sun and sky radiance measurements, Journal of Geophysical Research: Atmospheres, 105, 20673–20696, https://doi.org/10.1029/2000JD900282, 2000.

Dubovik, O., Smirnov, A., Holben, B. N., King, M. D., Kaufman, Y. J., Eck, T. F., and Slutsker, I.: Accuracy assessments of aerosol optical properties retrieved from Aerosol Robotic Network (AERONET) Sun and sky radiance measurements, Journal of Geophysical Research: Atmospheres, 105, 9791–9806, https://doi.org/10.1029/2000JD900040, 2000.

Dubovik, O., Holben, B., Eck, T. F., Smirnov, A., Kaufman, Y. J., King, M. D., Tanré, D., and Slutsker, I.: Variability of Absorption and Optical Properties of Key Aerosol Types Observed in Worldwide Locations, J Atmos Sci, 59, 590–608, https://doi.org/10.1175/1520-0469(2002)059<0590:VOAAOP>2.0.CO;2, 2002.

Dubovik, O., Sinyuk, A., Lapyonok, T., Holben, B. N., Mishchenko, M., Yang, P., Eck, T. F., Volten, H., Muñoz, O., Veihelmann, B., van der Zande, W. J., Leon, J.-F., Sorokin, M., and Slutsker, I.: Application of spheroid models to account for aerosol particle nonsphericity in remote sensing of desert dust, J Geophys Res, 111, D11208, https://doi.org/10.1029/2005JD006619, 2006.

Dubovik, O., Herman, M., Holdak, A., Lapyonok, T., Tanré, D., Deuzé, J. L., Ducos, F., Sinyuk, A., and Lopatin, A.: Statistically optimized inversion algorithm for enhanced retrieval of aerosol properties from spectral multi-angle polarimetric satellite observations, Atmos Meas Tech, 4, 975–1018, https://doi.org/10.5194/amt-4-975-2011, 2011.

Dubovik, O., Lapyonok, T., Litvinov, P., Herman, M., Fuertes, D., Ducos, F., Torres, B., Derimian, Y., Huang, X., Lopatin, A., Chaikovsky, A., Aspetsberger, M., and Federspiel, C.: GRASP: a versatile algorithm for characterizing the atmosphere, SPIE Newsroom, https://doi.org/10.1117/2.1201408.005558, 2014.

Dubovik, O., Li, Z., Mishchenko, M. I., Tanré, D., Karol, Y., Bojkov, B., Cairns, B., Diner, D. J., Espinosa, W. R., Goloub, P., Gu, X., Hasekamp, O., Hong, J., Hou, W., Knobelspiesse, K. D., Landgraf, J., Li, L., Litvinov, P., Liu, Y., Lopatin, A., Marbach, T., Maring, H., Martins, V., Meijer, Y., Milinevsky, G., Mukai, S., Parol, F., Qiao, Y., Remer, L., Rietjens, J., Sano, I., Stammes, P., Stamnes, S., Sun, X., Tabary, P., Travis, L. D., Waquet, F., Xu, F., Yan, C., and Yin, D.: Polarimetric remote sensing of atmospheric aerosols: Instruments, methodologies, results, and perspectives, J Quant Spectrosc Radiat Transf, 224, 474–511, https://doi.org/10.1016/J.JQSRT.2018.11.024, 2019.

Dubovik, O., Fuertes, D., Lytvynov, P., Lopatin, A., Lapyonok, T., Doubovik, I., Xu, F., Ducos, F., Chen, C., Torres, B., Derimian, Y., Li, L., Herrera, M., Karol, Y., Matar, C., Schuster, G., Espinosa, R., Puthukkudy, A., Li, Z., Juergen, F., Preusker, R., Cuesta, J., Kreuter, A., Cede, A., Aspetsberger, M., Marth, D., Bindreiter, L., Hangler, A., Lanzinger, V., Holter, C., and Federspiel, C.: A Comprehensive Description of Multi-Term LSM for Applying Multiple a Priori Constraints in Problems of Atmospheric Remote Sensing: GRASP Algorithm, Concept, and Applications, Frontiers in Remote Sensing, 1–23, https://doi.org/10.3389/FRSEN.2021.706851, 2021a.

Dubovik, O., Schuster, G. L., Xu, F., Hu, Y., Bösch, H., Landgraf, J., and Li, Z.: Grand Challenges in Satellite Remote

Sensing, Frontiers in Remote Sensing, 2, 619818, https://doi.org/10.3389/frsen.2020.603650, 2021b.

Frouin, R. and Pelletier, B.: Bayesian methodology for inverting satellite ocean-color data, Remote Sens Environ, 159, 332–360, https://doi.org/10.1016/J.RSE.2014.12.001, 2015.

Frouin, R., Schwindling, M., and Deschamps, P. Y.: Spectral reflectance of sea foam in the visible and near-infrared: In situ measurements and remote sensing implications, Journal of Geophysical Research C: Oceans, 101, 14361–14371, https://doi.org/10.1029/96JC00629, 1996.

Fu, G. and Hasekamp, O.: Retrieval of aerosol microphysical and optical properties over land using a multimode approach, Atmos Meas Tech, 11, 6627–6650, https://doi.org/10.5194/amt-11-6627-2018, 2018.

Fu, G., Hasekamp, O., Rietjens, J., Smit, M., Di Noia, A., Cairns, B., Wasilewski, A., Diner, D., Seidel, F., Xu, F., Knobelspiesse, K., Gao, M., da Silva, A., Burton, S., Hostetler, C., Hair, J., and Ferrare, R.: Aerosol retrievals from different polarimeters during the ACEPOL campaign using a common retrieval algorithm, Atmos Meas Tech, 13, 553–573, https://doi.org/10.5194/amt-13-553-2020, 2020.

Fuertes, D., Dubovik, O., Remer, L. A., Martin, V. J., Kleidman, R., and Federspiel, C.: The first commercial multi-angle polarimeter constellation: The GAPMAP mission, AGUFM, 2023, A53H-2353, 2023.

Gao, M., Zhai, P. W., Franz, B. A., Hu, Y., Knobelspiesse, K., Jeremy Werdell, P., Ibrahim, A., Cairns, B., and Chase, A.: Inversion of multiangular polarimetric measurements over open and coastal ocean waters: A joint retrieval algorithm for aerosol and water-leaving radiance properties, Atmos Meas Tech, 12, 3921–3941, https://doi.org/10.5194/AMT-12-3921-2019, 2019.

Ge, B., Li, Z., Chen, C., Hou, W., Xie, Y., Zhu, S., Qie, L., Zhang, Y., Li, K., Xu, H., Ma, Y., Yan, L., and Mei, X.: An Improved Aerosol Optical Depth Retrieval Algorithm for Multiangle Directional Polarimetric Camera (DPC), Remote Sens (Basel), 14, 4045, https://doi.org/10.3390/rs14164045, 2022.

Giles, D. M., Sinyuk, A., Sorokin, M. G., Schafer, J. S., Smirnov, A., Slutsker, I., Eck, T. F., Holben, B. N., Lewis, J. R., Campbell, J. R., Welton, E. J., Korkin, S. V., and Lyapustin, A. I.: Advancements in the Aerosol Robotic Network (AERONET) Version 3 database – automated near-real-time quality control algorithm with improved cloud screening for Sun photometer aerosol optical depth (AOD) measurements, Atmos Meas Tech, 12, 169–209, https://doi.org/10.5194/amt-12-169-2019, 2019.

Gu, X. and Tong, X.: Overview of China Earth Observation Satellite Programs [Space Agencies], IEEE Geosci Remote Sens Mag, 3, https://doi.org/10.1109/MGRS.2015.2467172, 2015.

Hansen, J., Sato, M., Lacis, A., and Ruedy, R.: The missing climate forcing, Philos Trans R Soc Lond B Biol Sci, 352, 231–240, https://doi.org/10.1098/RSTB.1997.0018, 1997.

Hasekamp, O., Litvinov, P., Fu, G., Chen, C., and Dubovik, O.: Algorithm evaluation for polarimetric remote sensing of atmospheric aerosols, Atmos Meas Tech, 17, 1497–1525, https://doi.org/10.5194/AMT-17-1497-2024, 2024.

Hasekamp, O. P., Litvinov, P., and Butz, A.: Aerosol properties over the ocean from PARASOL multiangle photopolarimetric measurements, J Geophys Res, 116, D14204, https://doi.org/10.1029/2010JD015469, 2011.

https://doi.org/10.5194/essd-2024-483
Preprint. Discussion started: 18 December 2024

Hasekamp, O. P., Fu, G., Rusli, S. P., Wu, L., Di Noia, A., Brugh, J. aan de, Landgraf, J., Martijn Smit, J., Rietjens, J., and van Amerongen, A.: Aerosol measurements by SPEXone on the NASA PACE mission: expected retrieval capabilities, J Quant Spectrosc Radiat Transf, 227, 170–184, https://doi.org/10.1016/j.jqsrt.2019.02.006, 2019.

Holben, B. N., Eck, T. F., Slutsker, I., Tanré, D., Buis, J. P., Setzer, A., Vermote, E., Reagan, J. A., Kaufman, Y. J., Nakajima, T., Lavenu, F., Jankowiak, I., and Smirnov, A.: AERONET—A Federated Instrument Network and Data Archive for Aerosol Characterization, Remote Sens Environ, 66, 1–16, https://doi.org/10.1016/S0034-4257(98)00031-5, 1998.

Hsu, N. C., Lee, J., Sayer, A. M., Kim, W., Bettenhausen, C., and Tsay, S. -C.: VIIRS Deep Blue Aerosol Products Over Land: Extending the EOS Long-Term Aerosol Data Records, Journal of Geophysical Research: Atmospheres, 124, 4026–4053, https://doi.org/10.1029/2018JD029688, 2019.

IPCC: Climate Change 2021: The Physical Science Basis. Contribution of Working Group I to the Sixth Assessment Report of the Intergovernmental Panel on Climate Change. edited by: Masson-Delmotte, V., et al. Cambridge University Press, (2021).

Jin, S., Ma, Y., Chen, C., Dubovik, O., Hong, J., Liu, B., and Gong, W.: Performance Evaluation for Retrieving Aerosol Optical Depth from Directional Polarimetric Camera (DPC) based on GRASP Algorithm, Atmos Meas Tech, 15, 4323–4337, https://doi.org/doi.org/10.5194/amt-15-4323-2022, 2022.

Knobelspiesse, K., Barbosa, H., Bradley, C., Bruegge, C., Cairns, B., Chen, G., Chowdhary, J., Cook, A., Di Noia, A., van Diedenhoven, B., Diner, D., Ferrare, R., Fu, G., Gao, M., Garay, M., Hair, J., Harper, D., van Harten, G., Hasekamp, O., Helmlinger, M., Hostetler, C., Kalashnikova, O., Kupchock, A., Longo De Freitas, K., Maring, H., Martins, J. V., McBride, B., McGill, M., Norlin, K., Puthukkudy, A., Rheingans, B., Rietjens, J., Seidel, F., da Silva, A., Smit, M., Stamnes, S., Tan, Q., Val, S., Wasilewski, A., Xu, F., Xu, X., and Yorks, J.: The Aerosol Characterization from Polarimeter and Lidar (ACEPOL) airborne field campaign, Earth Syst Sci Data, 2, 1–38, https://doi.org/10.5194/essd-2020-76, 2020.

Lei, X., Lei, X., Lei, X., Lei, X., Zhu, S., Zhu, S., Zhu, S., Li, Z., Li, Z., Hong, J., Hong, J., Liu, Z., Liu, Z., Liu, Z., Tao, F., Tao, F., Zou, P., Zou, P., Song, M., Song, M., Li, C., and Li, C.: Integration model of POSP measurement spatial response function, Optics Express, Vol. 28, Issue 17, pp. 25480-25489, 28, 25480–25489, https://doi.org/10.1364/OE.393897, 2020.

Lei, X., Liu, Z., Tao, F., Dong, H., Hou, W., Xiang, G., Qie, L., Meng, B., Li, C., Chen, F., Xie, Y., Zhang, M., Fan, L., Cheng, L., and Hong, J.: Data Comparison and Cross-Calibration between Level 1 Products of DPC and POSP Onboard the Chinese GaoFen-5(02) Satellite, Remote Sensing 2023, Vol. 15, Page 1933, 15, 1933, https://doi.org/10.3390/RS15071933, 2023.

Li, J., Ma, J., Li, C., Wang, Y., Li, Z., and Hong, J.: Multi-information collaborative cloud identification algorithm in Gaofen-5 Directional Polarimetric Camera imagery, J Quant Spectrosc Radiat Transf, 261, 107439, https://doi.org/10.1016/J.JQSRT.2020.107439, 2021.

https://doi.org/10.5194/essd-2024-483
Preprint. Discussion started: 18 December 2024

675 Li, L., Dubovik, O., Derimian, Y., Schuster, G. L., Lapyonok, T., Litvinov, P., Ducos, F., Fuertes, D., Chen, C., Li, Z., Lopatin, A., Torres, B., and Che, H.: Retrieval of aerosol components directly from satellite and ground-based measurements, Atmos Chem Phys, 19, 13409–13443, https://doi.org/10.5194/acp-19-13409-2019, 2019.

Li, L., Che, H., Zhang, X., Chen, C., Chen, X., Gui, K., Liang, Y., Wang, F., Derimian, Y., Fuertes, D., Dubovik, O., Zheng, Y., Zhang, L., Guo, B., Wang, Y., and Zhang, X.: A satellite-measured view of aerosol component content and optical 680 property in a haze-polluted case over North China Plain, Atmos Res, 266, 105958, https://doi.org/10.1016/J.ATMOSRES.2021.105958, 2022a.

Li, X. and Strahler, A. H.: Geometric-Optical Bidirectional Reflectance Modeling of the Discrete Crown Vegetation Canopy: Effect of Crown Shape and Mutual Shadowing, IEEE Transactions on Geoscience and Remote Sensing, 30, 276–292, https://doi.org/10.1109/36.134078, 1992.

685 Li, Z., Hou, W., Hong, J., Zheng, F., Luo, D., Wang, J., Gu, X., and Qiao, Y.: Directional Polarimetric Camera (DPC): Monitoring aerosol spectral optical properties over land from satellite observation, J Quant Spectrosc Radiat Transf, 218, 21–37, https://doi.org/10.1016/J.JQSRT.2018.07.003, 2018.

Li, Z., Xie, Y., Hou, W., Liu, Z., Bai, Z., Hong, J., Ma, Y., Huang, H., Lei, X., Sun, X., Liu, X., Yang, B., Qiao, Y., Zhu, J., Cong, Q., Zheng, Y., Song, M., Zou, P., Hu, Z., Lin, J., and Fan, L.: In-Orbit Test of the Polarized Scanning 690 Atmospheric Corrector (PSAC) Onboard Chinese Environmental Protection and Disaster Monitoring Satellite Constellation HJ-2 A/B, IEEE Transactions on Geoscience and Remote Sensing, 60, https://doi.org/10.1109/TGRS.2022.3176978, 2022b.

Li, Z., Hou, W., Qiu, Z., Ge, B., Xie, Y., Hong, J., Ma, Y., Peng, Z., Fang, W., Zhang, D., Sun, X., Qiao, Y., Yu, J., Yang, W., Lin, J., and Hu, Z.: Preliminary On-Orbit Performance Test of the First Polarimetric Synchronization Monitoring 695 Atmospheric Corrector (SMAC) On-Board High-Spatial Resolution Satellite Gao Fen Duo Mo (GFDM), IEEE Transactions on Geoscience and Remote Sensing, 60, https://doi.org/10.1109/TGRS.2021.3110320, 2022c.

Li, Z., Hou, W., Hong, J., Fan, C., Wei, Y., Liu, Z., Lei, X., Qiao, Y., Hasekamp, O. P., Fu, G., Wang, J., Dubovik, O., Qie, L. L., Zhang, Y., Xu, H., Xie, Y., Song, M., Zou, P., Luo, D., Wang, Y., and Tu, B.: The polarization crossfire (PCF) sensor suite focusing on satellite remote sensing of fine particulate matter PM2.5 from space, J Quant Spectrosc Radiat 700 Transf, 286, 108217, https://doi.org/10.1016/J.JQSRT.2022.108217, 2022d.

Litvinov, P., Hasekamp, O., Cairns, B., and Mishchenko, M.: Reflection models for soil and vegetation surfaces from multiple-viewing angle photopolarimetric measurements, J Quant Spectrosc Radiat Transf, 111, 529–539, https://doi.org/https://doi.org/10.1016/j.jqsrt.2009.11.001, 2010.

Litvinov, P., Hasekamp, O., and Cairns, B.: Models for surface reflection of radiance and polarized radiance: Comparison 705 with airborne multi-angle photopolarimetric measurements and implications for modeling top-of-atmosphere measurements, Remote Sens Environ, 115, 781–792, https://doi.org/10.1016/J.RSE.2010.11.005, 2011a.

Litvinov, P., Hasekamp, O., Cairns, B., and Mishchenko, M.: Semi-empirical BRDF and BPDF models applied to the problem of aerosol retrievals over land: testing on airborne data and implications for modeling of top-of-atmosphere

https://doi.org/10.5194/essd-2024-483
Preprint. Discussion started: 18 December 2024

measurements, in: Polarimetric Detection, Characterization and Remote Sensing, Springer, Dordrecht, 313–340, https://doi.org/10.1007/978-94-007-1636-0_13, 2011b.

Litvinov, P., Chen, C., Dubovik, O., Fuertes, D., Bindreiter, L., Lanzinger, V., de Graaf, M., Tilstra, G., Stammes, P.: S5p+Innovation AOD/BRDF Final Report, GRASP/KNMI, Issue 1.0, https://d37onar3vnbj2y.cloudfront.net/static/surface/albedo/documents/S5p%2BInnovation_AOD_BRDF_Final_Report_v1.1.pdf, 2022.

Litvinov, P., Chen, C., Dubovik, O., Bindreiter, L., Matar, C., Fuertes, D., Lopatin, A., Lapyonok, T., Lanzinger, V., Hangler, A., Aspetsberger, M., de Graaf, M., Tilstra, L. G., Stammes, P., Dandocsi, A., Gasbarra, D., Fluck, E., Zehner, C., and Retscher, C.: Extended aerosol and surface characterization from S5P/TROPOMI with GRASP algorithm. Part I: Conditions, approaches, performance and new possibilities, Remote Sens Environ, 313, 114355, https://doi.org/10.1016/J.RSE.2024.114355, 2024.

Lopatin, A., Dubovik, O., Fuertes, D., Stenchikov, G., Lapyonok, T., Veselovskii, I., Wienhold, F., Shevchenko, I., Hu, Q., and Parajuli, S.: Synergy processing of diverse ground-based remote sensing and in situ data using GRASP algorithm: applications to radiometer, lidar and radiosonde observations, Atmos Meas Tech, 14, 2575–2614, https://doi.org/10.5194/amt-14-2575-2021, 2021.

Maignan, F., Bréon, F. M., Fédèle, E., and Bouvier, M.: Polarized reflectances of natural surfaces: Spaceborne measurements and analytical modeling, Remote Sens Environ, 113, 2642–2650, https://doi.org/10.1016/j.rse.2009.07.022, 2009.

Martins, J., Kleidman, R., Remer, L., Dubovik, O., Fuertes, D., and Giralda, M. H.: The Climate-n Constellation of Small Satellites for the Detailed Measurement of Aerosol Pollution, Cloud Properties, and Greenhouse Gases, Small Satellite Conference, 2024.

Martins, J. V., Tanré, D., Remer, L., Kaufman, Y., Mattoo, S., and Levy, R.: MODIS Cloud screening for remote sensing of aerosols over oceans using spatial variability, Geophys Res Lett, 29, 8009, https://doi.org/10.1029/2001GL013252, 2002.

Martins, J. V., Fernandez-Borda, R., McBride, B., Remer, L., and Barbosa, H. M. J.: The harp hyperangular imaging polarimeter and the need for small satellite payloads with high science payoff for earth science remote sensing, International Geoscience and Remote Sensing Symposium (IGARSS), 2018-July, 6304–6307, https://doi.org/10.1109/IGARSS.2018.8518823, 2018.

Mishchenko, M. I., Cairns, B., Hansen, J. E., Travis, L. D., Burg, R., Kaufman, Y. J., Martins, J. V., and Shettle, E. P.: Monitoring of aerosol forcing of climate from space: Analysis of measurement requirements, J Quant Spectrosc Radiat Transf, 88, 149–161, https://doi.org/10.1016/j.jqsrt.2004.03.030, 2004.

Mishchenko, M. I., Cairns, B., Hansen, J. E., Travis, L. D., Kopp, G., Schueler, C. F., Fafaul, B. A., Hooker, R. J., Maring, H. B., Itchkawich, T., Mishchenko, M. I., Cairns, B., Hansen, J. E., Travis, L. D., Kopp, G., Schueler, C. F., Fafaul, B. A., Hooker, R. J., Maring, H. B., and Itchkawich, T.: Accurate Monitoring of Terrestrial Aerosols and Total Solar

https://doi.org/10.5194/essd-2024-483
Preprint. Discussion started: 18 December 2024

Irradiance: Introducing the Glory Mission, Bull Am Meteorol Soc, 88, 677–691, https://doi.org/10.1175/BAMS-88-5-677, 2007.

Monahan, E. C. and O'Muircheartaigh, L.: Optimal Power-Law Description of Oceanic Whitecap Coverage Dependence on Wind Speed, J Phys Oceanogr, 10, 2094–2099, https://doi.org/10.1175/1520-0485(1980)010<2094:OPLDOO>2.0.CO;2, 1980.

O'Neill, N. T., Eck, T. F., Smirnov, A., Holben, B. N., and Thulasiraman, S.: Spectral discrimination of coarse and fine mode optical depth, Journal of Geophysical Research D: Atmospheres, 108, https://doi.org/10.1029/2002jd002975, 2003.

Remer, L. A., Davis, A. B., Mattoo, S., Levy, R. C., Kalashnikova, O. V., Coddington, O., Chowdhary, J., Knobelspiesse, K., Xu, X., Ahmad, Z., Boss, E., Cairns, B., Dierssen, H. M., Diner, D. J., Franz, B., Frouin, R., Gao, B.-C., Ibrahim, A., Martins, J. V., Omar, A. H., Torres, O., Xu, F., and Zhai, P.-W.: Retrieving Aerosol Characteristics From the PACE Mission, Part 1: Ocean Color Instrument, Front Earth Sci (Lausanne), 7, 152, https://doi.org/10.3389/feart.2019.00152, 2019a.

Remer, L. A., Knobelspiesse, K., Zhai, P.-W., Xu, F., Kalashnikova, O. V., Chowdhary, J., Hasekamp, O., Dubovik, O., Wu, L., Ahmad, Z., Boss, E., Cairns, B., Coddington, O., Davis, A. B., Dierssen, H. M., Diner, D. J., Franz, B., Frouin, R., Gao, B.-C., Ibrahim, A., Levy, R. C., Martins, J. V., Omar, A. H., and Torres, O.: Retrieving Aerosol Characteristics From the PACE Mission, Part 2: Multi-Angle and Polarimetry, Front Environ Sci, 7, 94, https://doi.org/10.3389/fenvs.2019.00094, 2019b.

Roujean, J. L., Leroy, M., and Deschamps, P. Y.: A bidirectional reflectance model of the Earth's surface for the correction of remote sensing data, Journal of Geophysical Research: Atmospheres, 97, 20455–20468, https://doi.org/10.1029/92JD01411, 1992.

Sayer, A. M., Hsu, N. C., Lee, J., Bettenhausen, C., Kim, W. V., and Smirnov, A.: Satellite Ocean Aerosol Retrieval (SOAR) Algorithm Extension to S-NPP VIIRS as Part of the "Deep Blue" Aerosol Project, Journal of Geophysical Research: Atmospheres, 123, 380–400, https://doi.org/10.1002/2017JD027412, 2018a.

Sayer, A. M., Hsu, N. C., Lee, J., Kim, W. V., Dubovik, O., Dutcher, S. T., Huang, D., Litvinov, P., Lyapustin, A., Tackett, J. L., and Winker, D. M.: Validation of SOAR VIIRS Over-Water Aerosol Retrievals and Context Within the Global Satellite Aerosol Data Record, Journal of Geophysical Research: Atmospheres, 123, 2018JD029465, https://doi.org/10.1029/2018JD029465, 2018b.

Schaaf, C., & Wang, Z. (2015b). MCD43C3 MODIS/Terra+Aqua BRDF/Albedo Albedo Daily L3 Global 0.05Deg CMG V006 [Data set]. NASA EOSDIS Land Processes DAAC. Accessed 2020-09-14 from https://doi.org/10.5067/MODIS/MCD43C3.006

Shang, H., Letu, H., Chen, L., Riedi, J., Ma, R., Wei, L., Labonnote, L. C., Hioki, S., Liu, C., Wang, Z., and Wang, J.: Cloud thermodynamic phase detection using a directional polarimetric camera (DPC), J Quant Spectrosc Radiat Transf, 253, 107179, https://doi.org/10.1016/J.JQSRT.2020.107179, 2020.

https://doi.org/10.5194/essd-2024-483
Preprint. Discussion started: 18 December 2024

Sinyuk, A., Holben, B. N., Eck, T. F., Giles, D. M., Slutsker, I., Korkin, S., Schafer, J. S., Smirnov, A., Sorokin, M., and Lyapustin, A.: The AERONET Version 3 aerosol retrieval algorithm, associated uncertainties and comparisons to Version 2, Atmos Meas Tech, 13, 3375–3411, https://doi.org/10.5194/amt-13-3375-2020, 2020.

Smirnov, A., Holben, B. N., Eck, T. F., Dubovik, O., and Slutsker, I.: Cloud-Screening and Quality Control Algorithms for the AERONET Database, Remote Sens Environ, 73, 337–349, https://doi.org/10.1016/S0034-4257(00)00109-7, 2000.

Tanré, D., Bréon, F. M., Deuzé, J. L., Dubovik, O., Ducos, F., François, P., Goloub, P., Herman, M., Lifermann, A., and Waquet, F.: Remote sensing of aerosols by using polarized, directional and spectral measurements within the A-Train: the PARASOL mission, Atmos Meas Tech, 4, 1383–1395, https://doi.org/10.5194/amt-4-1383-2011, 2011.

Tong, X., Zhao, W., Xing, J., and Fu, W.: Status and development of China High-Resolution Earth Observation System and application, International Geoscience and Remote Sensing Symposium (IGARSS), 2016-November, 3738–3741, https://doi.org/10.1109/IGARSS.2016.7729969, 2016.

Voss, K. J., Morel, A., and Antoine, D.: Detailed validation of the bidirectional effect in various Case 1 waters for application to ocean color imagery, Biogeosciences, 4, 781–789, https://doi.org/10.5194/BG-4-781-2007, 2007.

Wang, S., Gong, W., Fang, L., Wang, W., Zhang, P., Lu, N., Tang, S., Zhang, X., Hu, X., and Sun, X.: Aerosol Retrieval over Land from the Directional Polarimetric Camera Aboard on GF-5, Atmosphere 2022, Vol. 13, Page 1884, 13, 1884, https://doi.org/10.3390/ATMOS13111884, 2022.

Wanner, W., Li, X., and Strahler, A. H.: On the derivation of kernels for kernel-driven models of bidirectional reflectance, Journal of Geophysical Research: Atmospheres, 100, 21077–21089, https://doi.org/10.1029/95JD02371, 1995.

Waquet, F., Cairns, B., Knobelspiesse, K., Chowdhary, J., Travis, L. D., Schmid, B., and Mishchenko, M. I.: Polarimetric remote sensing of aerosols over land, Journal of Geophysical Research Atmospheres, 114, https://doi.org/10.1029/2008JD010619, 2009.

Xu, F., Dubovik, O., Zhai, P. W., Diner, D. J., Kalashnikova, O. V., Seidel, F. C., Litvinov, P., Bovchaliuk, A., Garay, M. J., Van Harten, G., and Davis, A. B.: Joint retrieval of aerosol and water-leaving radiance from multispectral, multiangular and polarimetric measurements over ocean, Atmos Meas Tech, 9, 2877–2907, https://doi.org/10.5194/AMT-9-2877-2016, 2016.

Xu, F., van Harten, G., Diner, D. J., Kalashnikova, O. V., Seidel, F. C., Bruegge, C. J., and Dubovik, O.: Coupled retrieval of aerosol properties and land surface reflection using the Airborne Multiangle SpectroPolarimetric Imager, Journal of Geophysical Research: Atmospheres, 122, 7004–7026, https://doi.org/10.1002/2017JD026776, 2017a.

Xu, F., van Harten, G., Diner, D. J., Kalashnikova, O. V., Seidel, F. C., Bruegge, C. J., and Dubovik, O.: Coupled retrieval of aerosol properties and land surface reflection using the Airborne Multiangle SpectroPolarimetric Imager, J Geophys Res, 122, 7004–7026, https://doi.org/10.1002/2017JD026776, 2017b.

Yu, H., Sun, X., Tu, B., Ti, R., Ma, J., Hong, J., Chen, C., Liu, X., Huang, H., Wang, Z., Ahmad, S., Wang, Y., Fan, Y., Li, Y., Wei, Y., Wang, Y., and Wang, Y.: Towards multi-views cloud retrieval accounting for the 3-D structure collected by directional polarization camera, ISPRS Journal of Photogrammetry and Remote Sensing, 212, 146–163,

https://doi.org/10.5194/essd-2024-483
Preprint. Discussion started: 18 December 2024

https://doi.org/10.1016/J.ISPRSJPRS.2024.04.028, 2024.

Zhang, R., Zhou, W., Chen, H., Zhang, L., Zhang, L., Ma, P., Zhao, S., and Wang, Z.: Aerosol Information Retrieval from GF-5B DPC Data over North China Using the Dark Dense Vegetation Algorithm, Atmosphere 2023, Vol. 14, Page 241, 14, 241, https://doi.org/10.3390/ATMOS14020241, 2023.